Available online at www.sciencedirect.com
ScienceDirect
Journal of Computational Physics 227 (2008) 6106–6139
JOURNAL OF COMPUTATIONAL PHYSICS
www.elsevier.com/locate/jcp

Computational high frequency waves through curved interfaces via the Liouville equation and geometric theory of diffraction ☆

Shi Jin [a,b], Dongsheng Yin [c,*]

[a] Department of Mathematical Sciences, Tsinghua University, Beijing 100084, PR China
[b] Department of Mathematics, University of Wisconsin, Madison, WI 53706, USA
[c] Department of Mathematical Sciences and the Center for Advanced Study, Tsinghua University, Beijing 100084, PR China

Received 1 December 2006; received in revised form 22 February 2008; accepted 22 February 2008
Available online 18 March 2008

Abstract

We construct a class of numerical schemes for the Liouville equation of geometric optics coupled with the Geometric Theory of Diffractions to simulate the high frequency linear waves with a discontinuous index of refraction. In this work [S. Jin, X. Wen, A Hamiltonian-preserving scheme for the Liouville equation of geometric optics with partial transmissions and reflections, SIAM J. Numer. Anal. 44 (2006) 1801–1828], a Hamiltonian-preserving scheme for the Liouville equation was constructed to capture partial transmissions and reflections at the interfaces. This scheme is extended by incorporating diffraction terms derived from Geometric Theory of Diffraction into the numerical flux in order to capture diffraction at the interface. We give such a scheme for curved interfaces. This scheme is proved to be positive under a suitable time step constraint. Numerical experiments show that it can capture diffraction phenomena without fully resolving the wave length of the original wave equation.

Keywords: High frequency waves; Liouville equation; Geometrical theory of diffraction; Geometric optics; Creeping wave; Numerical methods

1. Introduction

In this paper, we construct a numerical scheme for the high frequency wave equation in two-dimension:

$$u_{tt} - c(\mathbf{x})^2 \Delta u = 0, \quad t > 0, \quad \mathbf{x} \in \Omega \subset R^2, \tag{1.1}$$

$$u(0) = A(\mathbf{x}, 0) \mathrm{e}^{\mathrm{i}\phi(\mathbf{x},0)/\epsilon}, \tag{1.2}$$

☆ Research supported in part by NSF Grant Nos. DMS-0305081 and DMS-0608720, and NSFC for Project 10228101, and China Postdoctoral Science Foundation 20060390076.
* Corresponding author.
E-mail addresses: jin@math.wisc.edu (S. Jin), dyin@math.tsinghua.edu.cn (D. Yin).

0021-9991/$ - see front matter © 2008 Elsevier Inc. All rights reserved.
doi:10.1016/j.jcp.2008.02.029

$$\frac{\partial u}{\partial t}(0) = B(\mathbf{x},0)e^{i\phi(\mathbf{x},0)/\epsilon} \tag{1.3}$$

with suitable boundary conditions on $\partial\Omega$. Here $c(\mathbf{x})$ is the local wave speed, and $\epsilon \ll 1$ is a parameter measuring the ratio of the wave length over the domain. In this problem, the relative wave length ϵ is very small, or the *essential frequencies* of the wave, which are of $O(1/\epsilon)$, are high. A direct simulation of the problem is prohibitively costly, thus approximate models for wave propagation based on geometric optics (GO) are usually used [13,16].

We are concerned with the case when $c(\mathbf{x})$ contains *discontinuities* due to different media. Note $n(x) = \frac{c_0}{c(\mathbf{x})}$, for c_0 a reference wave speed, is the index of refraction which is different in different media. This discontinuity will generate an *interface*, and as a consequence waves crossing this interface will undergo transmissions, reflections and diffractions.

One of the approximate models for high frequency wave equation is the Liouville equation, which arises in phase space description of geometric optics (GO) [13]:

$$f_t + H_{\mathbf{k}} \cdot \nabla_{\mathbf{x}} f - H_{\mathbf{x}} \cdot \nabla_{\mathbf{k}} f = 0, \quad t > 0, \quad \mathbf{x}, \mathbf{k} \in R^d, \tag{1.4}$$

where $f(t, \mathbf{x}, \mathbf{k})$ is the energy density distribution of waves depending on position $\mathbf{x}$, time t and slowness vector $\mathbf{k}$, while the Hamiltonian H possesses the form

$$H(\mathbf{x}, \mathbf{k}) = c(\mathbf{x})|\mathbf{k}| = c(\mathbf{x})\sqrt{k_1^2 + k_2^2 + \cdots + k_d^2}. \tag{1.5}$$

The bicharacteristics of this Liouville equation (1.4) satisfies the Hamiltonian systems:

$$\frac{d\mathbf{x}}{dt} = c(\mathbf{x})\frac{\mathbf{k}}{|\mathbf{k}|}, \frac{d\mathbf{k}}{dt} = -c_{\mathbf{x}}|\mathbf{k}|. \tag{1.6}$$

In classical mechanics the Hamiltonian (1.5) of a particle remains a constant along particle trajectory, when it is being transmitted and reflected by the interface.

Recently several phase space based level set methods for high frequency waves, in particular the multivalued solutions in GO are based on this equation, see [6,14,17,18,22,23,27,37]. Semiclassical limit of wave equation with transmissions and reflections at the interface were studied in [1,32,39]. A Liouville equation based level set method for the wave front, but with only reflection, was introduced in [9]. See also a higher order method for multiple reflection [10].

In [26], a class of Hamiltonian-preserving numerical schemes for the Liouville equation (1.4) with partial transmissions and reflections was constructed. The design principle there was to build the behavior of the wave at the interface—either cross over with a changed velocity (or momentum) according to a constant Hamiltonian or be reflected with a negative velocity—into the numerical flux. See also earlier works [24,25]. These schemes are called *Hamiltonian-preserving schemes*, since they use a constant Hamiltonian to determine particle velocity on one side of the interface from the other side in the case of transmission. It gives a criterion for a unique solution to the governing Liouville equation (1.4), which is linearly hyperbolic with singular (discontinuous or measure-valued) coefficients. For a plane wave hitting an interface, it selects the solution that describes the interface condition in GO governed by *Snell's Law of refraction* when the interface width is much shorter than the wave length, namely a sharp interface.

Previously many numerical methods have been introduced to compute effectively wave propagations through heterogeneous media, including acoustic waves and elastic waves, see [31,45] and references therein. The *Hamiltonian-preserving* scheme bears some similarity with the immersed interface method [45], in that the interface condition is built into the numerical flux. Unlike these earlier works, which were most effective for low frequency waves, the *Hamiltonian-preserving* scheme is advantageous for high frequency waves. Using the high frequency limit—the Liouville equation—our numerical methods do not need to fully resolve the short wave length.

The derivation of GO does not take into account the effects of geometry and boundary conditions, which give rise to GO solutions that are discontinuous. Diffractions are lost in the infinite frequency approximation such as the Liouville equation. In this case, correction terms can be derived, as done in *Geometric Theory of Diffraction* (GTD) by Keller in [28]. GTD provides a systematic technique for adding diffraction effect to the GO approximations.

The aim of this paper is to construct a numerical scheme that accounts for transmission, reflection *and diffraction*, when computable transmission, reflection, and diffraction coefficients are available. The idea is to modify the numerical flux of [26] to include terms responsible for diffractions. These new terms incorporate GTD theory, including diffraction coefficients and decay rates of the surface waves. In this direction, we mention recent numerical methods for creeping waves [35,36,43]. To our knowledge, our method is the first Eulerian method for diffraction at interfaces that takes into consideration of partial transmissions, reflections and diffractions. We develop such a scheme for curved interfaces. Other geometries will be studied in our future works.

This paper is organized as follows: the GO approximations by the Wigner transform and by the WKB expansion for wave equation are presented in Section 2. In Section 3, we illustrate the behavior of waves at curved interfaces. We give detailed descriptions of GTD for two types of curved interfaces. In Section 4, interface conditions for (1.4) that incorporate transmission, reflection and diffraction coefficients are introduced. We then build these new interface conditions into the numerical fluxes and describe the numerical method in Section 5. Numerical examples are given in Section 6 to verify the accuracy of the scheme against the full simulation based on the wave equation (1.1)–(1.3). Finally, we make some concluding remarks in Section 7. The detailed algorithms are documented in the Appendix.

2. Geometric optics approximation of the wave equation in the phase space

Consider the two-dimensional wave equation

$$u_{tt} - c(\mathbf{x})^2 \Delta u = 0, \quad \mathbf{x} \in R^2, \ t \in R, \tag{2.1}$$

$$u|_{t=0} = u_I, \quad u_t|_{t=0} = s_I. \tag{2.2}$$

Introduce the new dependent variables

$$s = u_t, \quad \mathbf{r} = \nabla u$$

to obtain the system

$$\begin{cases} \frac{\partial \mathbf{r}}{\partial t} - \nabla s = 0, \\ \frac{1}{c(\mathbf{x})^2} \frac{\partial s}{\partial t} - \mathrm{div}\mathbf{r} = 0. \end{cases} \tag{2.3}$$

The energy density is given by

$$\mathcal{E}(\mathbf{x}, t) = \frac{1}{2} \frac{1}{c(\mathbf{x})^2} |u_t|^2 + \frac{1}{2} |\nabla u|^2. \tag{2.4}$$

Let $\mathbf{w} = \left(\frac{\partial u}{\partial x_1}, \frac{\partial u}{\partial x_2}, s \right)$. Then system (2.3) can be put in the form of a symmetric hyperbolic system

$$A(\mathbf{x}) \frac{\partial \mathbf{w}}{\partial t} + \sum_i D_i \frac{\partial \mathbf{w}}{\partial x_i} = 0 \tag{2.5}$$

with initial data

$$\mathbf{w}(0, \mathbf{x}) = \mathbf{w}_0(\mathbf{x}).$$

The matrix $A(\mathbf{x}) = \mathrm{diag}(1, 1, \frac{1}{c(\mathbf{x})^2})$, where each of the matrices D_i is constant and symmetric with entries either 0 or -1.

To study the GO limit of solution of (2.5), we assume that the coefficients of the matrix $A(\mathbf{x})$ vary on a scale much longer than the scale on which the initial data vary. Let ϵ be the ratio of these two scales. Rescaling space and time coordinates $(\mathbf{x}, t)$ by $\mathbf{x} \to \epsilon \mathbf{x}, t \to \epsilon t$, one obtains

$$A(\mathbf{x}) \frac{\partial \mathbf{w}^\epsilon}{\partial t} + \sum_i D_i \frac{\partial \mathbf{w}^\epsilon}{\partial x_i} = 0, \tag{2.6}$$

$$\mathbf{w}^\epsilon(0, \mathbf{x}) = \mathbf{w}_0\left(\frac{\mathbf{x}}{\epsilon}\right) \quad \text{or} \quad \mathbf{w}_0\left(\frac{\mathbf{x}}{\epsilon}, \mathbf{x}\right). \tag{2.7}$$

Note that the parameter ϵ does not appear explicitly in (2.6). It enters through the initial data (2.7). We are interested in the initial data of the standard GO form

$$\mathbf{w}^\epsilon(0,\mathbf{x}) = A_0(\mathbf{x})\mathrm{e}^{\mathrm{i}S_0(x)/\epsilon}. \tag{2.8}$$

Following [38], one can study the GO limit of (2.6) by using the Wigner distribution matrix W^ϵ:

$$W^\epsilon(t,\mathbf{x},\mathbf{k}) = \left(\frac{1}{2\pi}\right)^2 \int \mathrm{e}^{\mathrm{i}\mathbf{k}\cdot\mathbf{y}}\mathbf{w}^\epsilon(t,\mathbf{x}-\epsilon\mathbf{y}/2)\overline{\mathbf{w}^\epsilon(\mathbf{x}+\epsilon\mathbf{y}/2)}^t \mathrm{d}\mathbf{y}, \tag{2.9}$$

where $\overline{\mathbf{w}}^t$ is the conjugate transpose of $\mathbf{w}$. Although W^ϵ is not positive definite, it becomes so as $\epsilon = 0$.

The energy density for (2.6) is given by

$$\mathcal{E}^\epsilon(t,\mathbf{x}) = \frac{1}{2}(A(\mathbf{x})\mathbf{w}^\epsilon(t,\mathbf{x}),\mathbf{w}^\epsilon(t,\mathbf{x})) = \frac{1}{2}\int \mathrm{Tr}(A(\mathbf{x})W^\epsilon(t,\mathbf{x},\mathbf{k}))\mathrm{d}\mathbf{k}. \tag{2.10}$$

Let

$$\lim_{\epsilon\to 0} W^\epsilon(t,\mathbf{x},\mathbf{k}) = W^{(0)}(t,\mathbf{x},\mathbf{k}).$$

As $\epsilon \to 0$, the high frequency limit of $\mathcal{E}^\epsilon(t,\mathbf{x})$ is

$$\mathcal{E}^{(0)}(t,\mathbf{x}) = \frac{1}{2}\int \mathrm{Tr}(A(\mathbf{x})W^{(0)}(t,\mathbf{x},\mathbf{k}))\mathrm{d}\mathbf{k} = \int a^+(t,\mathbf{x},\mathbf{k})\mathrm{d}\mathbf{k}, \tag{2.11}$$

where the amplitude $a^\pm(t,\mathbf{x},\mathbf{k})$ is given by

$$a^\pm(t,\mathbf{x},\mathbf{k}) = \frac{1}{(2\pi)^2}\int \mathrm{d}\mathbf{y}\mathrm{e}^{\mathrm{i}\mathbf{k}\cdot\mathbf{y}} f_\pm(t,\mathbf{x},\mathbf{x}-\mathbf{y}/2,\mathbf{k})\overline{f_\pm(t,\mathbf{x},\mathbf{x}+\mathbf{y}/2,\mathbf{k})} \tag{2.12}$$

with

$$f_\pm(t,\mathbf{x},\mathbf{z},\mathbf{k}) = \sqrt{\frac{1}{2}}(\nabla u(t,\mathbf{z})\cdot\hat{\mathbf{k}}) \pm \frac{\sqrt{2}}{2|c(\mathbf{x})|}\frac{\partial u}{\partial t}(t,\mathbf{z}) \tag{2.13}$$

and $\hat{\mathbf{k}} = \mathbf{k}/|\mathbf{k}| = (\cos\theta,\sin\theta)^t$. This shows that

$$a^+(t,\mathbf{x},\mathbf{k}) = a^-(t,\mathbf{x},-\mathbf{k}) \tag{2.14}$$

and therefore one needs only to keep track of $a^+(t,\mathbf{x},\mathbf{k})$. It satisfies the Liouville equation [38]

$$\frac{\partial a^+}{\partial t} + c(\mathbf{x})\hat{\mathbf{k}}\cdot\nabla_{\mathbf{x}}a^+ - |\mathbf{k}|\nabla_{\mathbf{x}}c(\mathbf{x})\cdot\nabla_{\mathbf{k}}a^+ = 0. \tag{2.15}$$

Therefore, a^+ can be interpreted as the phase space energy density distribution. It solves the Liouville equations (1.4) and (1.5), with the zeroth moment giving the spatial energy density $\mathcal{E}^{(0)}(t,\mathbf{x})$ as in (2.11).

Next we mention the connection with the usual WKB approximation. We look for a solution of (2.6) with the initial data

$$\mathbf{w}(0,\mathbf{x}) = \mathbf{w}_0(\mathbf{x})\mathrm{e}^{\mathrm{i}S_0(\mathbf{x})/\epsilon}, \tag{2.16}$$

in the form

$$\mathbf{w}(t,\mathbf{x}) = (A_0(t,\mathbf{x}) + \epsilon A_1\cdots)\mathrm{e}^{\mathrm{i}S(t,\mathbf{x})/\epsilon} \tag{2.17}$$

with $A_0 = (\mathbf{r}_0, s_0)$. The leading order in ϵ gives the eiconal equation for the phase S

$$\frac{1}{c(\mathbf{x})^2}S_t^2 - (\nabla S)^2 = 0. \tag{2.18}$$

The next term $\mathrm{O}(\epsilon^2)$ yields the transport equation satisfied by the amplitude $\mathcal{A}(\mathbf{x},t)$,

$$\frac{\partial}{\partial t}|\mathcal{A}|^2 + \nabla\cdot\left(|\mathcal{A}|^2|c(\mathbf{x})|\frac{\nabla S}{|\nabla S|}\right) = 0. \tag{2.19}$$

It can be rewritten in conservative form

$$\frac{\partial}{\partial t}|\mathcal{A}|^2 + \nabla \cdot (|\mathcal{A}|^2 \nabla_{\mathbf{k}} H(\mathbf{x}, \nabla S)) = 0. \tag{2.20}$$

The eiconal and transport equations (2.18) and (2.19) can also be derived from (2.15) as follows. In the GO limit, initial data of form (2.16) implies that

$$a^+(0, \mathbf{x}, \mathbf{k}) = |\mathcal{A}_0(\mathbf{x})|^2 \delta(\mathbf{k} - \nabla S_0(\mathbf{x})). \tag{2.21}$$

Let the functions $S(t, \mathbf{x})$ and $|\mathcal{A}(t, \mathbf{x})|^2$ be the solutions of the eiconal and transport equations (2.18) and (2.19), respectively, with initial conditions $S(0, \mathbf{x}) = S_0(\mathbf{x})$ and $\mathcal{A}(0, \mathbf{x}) = \mathcal{A}_0(\mathbf{x})$. Then the solution of the Liouville equation (2.15) is

$$a^+(t, \mathbf{x}, \mathbf{k}) = |\mathcal{A}(t, \mathbf{x})|^2 \delta(\mathbf{k} - \nabla S(t, \mathbf{x})). \tag{2.22}$$

Conversely, given initial conditions of the form (2.21) for (2.15) and a^+ by (2.22), S and $\mathcal{A}$ must satisfy the eiconal and transport equations respectively by taking the zeroth and first moments of the Liouville equation (2.15). This shows that one can recover the WKB approximation from the Liouville equation. However, the WKB approximation breaks down at caustics, where the velocity ∇S is discontinuous and the amplitude $|A|$ is unbounded. Beyond the caustics, a computation based on the eiconal equation and the transport equation picks up the so-called viscosity solution [12], while the physical GO solution to the eiconal and transport equations becomes multi-valued [20,42].

The GO approximation is good when ϵ is very small. For moderately small ϵ, diffraction cannot be ignored. Clearly, the Liouville equation (2.15), valid at $\epsilon = 0$, contains no information about transmission and reflection—which occur even for $\epsilon = 0$, nor any information about diffraction which occurs for $\epsilon > 0$. It is not valid at the interface.

In the next section, we will discuss the behavior of waves at curved interfaces.

3. The behavior of waves at an interface

3.1. Transmission and reflection

In GO, when a wave propagates with its energy density governed by the Liouville equation (1.4), its Hamiltonian $H = c|\mathbf{k}|$ should be preserved across the interface:

$$H(c^+, \mathbf{k}_i) = H(c^+, \mathbf{k}_r) = H(c^-, \mathbf{k}_t), \tag{3.1}$$

where the superscripts "$\pm$" indicate the one-sided limits of wave speed at the interface, and $\mathbf{k}_i, \mathbf{k}_r$ and $\mathbf{k}_t$ denote the velocities of incident waves, reflected waves and transmitted waves, respectively. The wave can be partly reflected and partly transmitted. The condition (3.1) can be used to determine the particle velocity on one side of the interface from its value on the other side. When a plane wave hits an interface, this condition is equivalent to *Snell's Law of refraction* [24]

$$\frac{\sin\theta_i}{c^-} = \frac{\sin\theta_t}{c^+} \tag{3.2}$$

(for a wave hits the interface from the left) and the reflection law

$$\theta_r = \theta_i, \tag{3.3}$$

where θ_i, θ_t and θ_r stand for angles of incident, transmitted and reflected waves. The reflection coefficient is given by (see for example [1,32,39]),

$$\alpha_{\pm}^{\mathrm{R}} = \left(\frac{c^{\pm}\cos\theta_i - c^{\mp}\cos\theta_t}{c^{\pm}\cos\theta_r + c^{\mp}\cos\theta_t}\right)^2, \tag{3.4}$$

while the transmission coefficient is $\alpha_{\pm}^{\mathrm{T}} = 1 - \alpha_{\pm}^{\mathrm{R}}$. Here $\alpha_{+}^{\mathrm{R}}, \alpha_{+}^{\mathrm{T}}$ are for the right moving wave while $\alpha_{-}^{\mathrm{R}}, \alpha_{-}^{\mathrm{T}}$ are for the left moving waves.

3.2. Diffraction

Assume $c^+ > c^-$. When a wave hits the interface from the slow medium, there is a critical angle θ_c at which the refracted wave is parallel to the interface, namely,

$$\sin\theta_c = \frac{c^-}{c^+}. \tag{3.5}$$

This critically refracted wave is a surface wave in the fast medium [3,29]. Consequently, it sheds refracted wave back into the slow medium. These shed waves are diffracted waves, which leave the interface at the critical angle at every point. Because the shed waves will carry energy, the surface waves will decay exponentially with the factor β, which is called the attenuation constant. The diffraction coefficient and the attenuation constant only depend on the local geometry, the relative wave length ϵ and the boundary conditions [30,33,40].

The behavior of the surface wave depends on the local curvature of the interface [7,8]. The local properties of the interface can be classified into two types:

- **Type A** interface: an interface convex towards the fast medium.
- **Type B** interface: an interface convex towards the slow medium.

Below we will only consider the case of $c^+ > c^-$. The other case can be obtained by interchanging the **Type A** interface with the **Type B** interface.

3.2.1. The *Type A* interface

For a **Type A** interface, a diffracted wave can be produced by the following two ways (see Fig. 1):

(I) An incident wave on the fast medium hits the interface *tangentially* (like GF). In this case, the incident wave will produce a surface wave along the fast side of the interface, which is called a "creeping wave". The creeping wave moves along the interface, continuously sheds *tangentially diffracted waves* into the fast medium (like BP_6) and *critically transmitted* waves into the slow medium (like EP_5).

(II) An incident wave on the slow medium hits the interface at a *critical* angle of incidence (like QB). The critically incident wave will produce a *critically reflected wave back to the slow medium* like BP_3, and a creeping wave on the fast side of the interface, along BCD, which sheds *tangentially diffracted waves* into the fast medium, like BP_6, and *critically diffracted waves* at the critical angle into the slow medium, like EP_5.

Let ϵ_+ denote the relative wavelength in the fast medium. In **case I**, since the shed waves will carry energy, the waves will decay exponentially. The attenuation constants is [34],

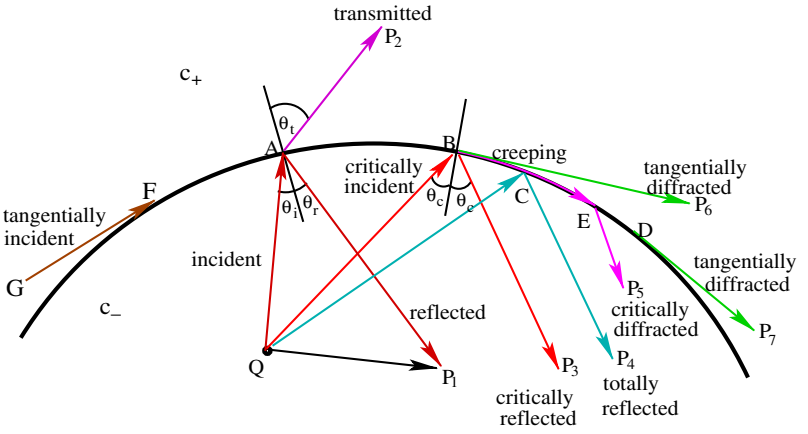

Fig. 1. Wave reflection, transmission and diffraction at a **Type A** interface.

$$\beta_{A_1} = \frac{\sqrt{3}}{2} q_0 \left(\frac{1}{2\epsilon_+}\right)^{1/3} (\rho^+ + 1/a)^{2/3} - \frac{\rho^+ + 1/a}{\sqrt{1/N^2 - 1}} \tag{3.6}$$

with $q_0 \approx 2.33811$ being the smallest positive zero of the Airy function which is given by

$$\mathrm{Ai}(-x) = \frac{1}{\pi} \int_0^\infty \cos\left(\frac{1}{2}\tau^3 - x\tau\right) \mathrm{d}\tau.$$

$N = c^-/c^+$, $\rho^\pm = |\nabla c^\pm(\mathbf{x})|/|c^\pm(\mathbf{x})|$ is the curvature of the diffracted rays at the diffracted point [30], a is the radius of curvature of the interface at the diffracted point.

In the vicinity of the interface, there exist boundary layers [5]. A boundary layer of thickness $\mathrm{O}(\epsilon_+^{2/3})$ is a narrow zone through which the waves undergo rapid variations. The diffraction coefficients outside the boundary layer is

$$\alpha^{\mathrm{D}}_{A_1^{\mathrm{o}}} = \frac{\pi^{1/2}}{2^{5/6}} [(\rho^+ + 1/a) r]^{-1/2} [(\rho^+ + 1/a)\epsilon_+]^{1/6} \frac{N^2}{[\mathrm{Ai}'(-q_0)]^2 [1 - N^2]}, \tag{3.7}$$

where r is the distance from the diffracted point, $\mathrm{Ai}'(-q) = 0$ is the derivative of the Airy function and the prime denotes the differentiation with respect to the argument of the Airy function. The diffraction coefficient $\alpha^{\mathrm{D}}_{A_1^{\mathrm{b}}}$ in the boundary layer is given by [34]

$$\alpha^{\mathrm{D}}_{A_1^{\mathrm{b}}} = \frac{\pi}{2} \frac{|\ \mathrm{Ai}(-\epsilon_+^{-2/3} 2^{1/3} (\rho^+ + 1/a)^{1/3} r + q_0 \mathrm{e}^{\mathrm{i}\pi/3})|}{[\ \mathrm{Ai}'(-q_0)]^2 [1/N^2 - 1]}. \tag{3.8}$$

Since the GO limit is not valid at the boundary layer, we cannot directly use $\alpha^{\mathrm{D}}_{A_1^{\mathrm{o}}}$. A reasonable choice of $\alpha^{\mathrm{D}}_{A_1}$ is to match the diffraction coefficients $\alpha^{\mathrm{D}}_{A_1^{\mathrm{o}}}$ and $\alpha^{\mathrm{D}}_{A_1^{\mathrm{b}}}$, which means to find r such that:

$$\alpha^{\mathrm{D}}_{A_1^{\mathrm{o}}} = \alpha^{\mathrm{D}}_{A_1^{\mathrm{b}}}.$$

Namely, we should find the smallest positive solution r_0 of the following equation:

$$s^{1/2} |\mathrm{Ai}(-\epsilon_+^{-2/3} 2^{1/3} (\rho^+ + 1/a)^{1/3} s + q_0 \mathrm{e}^{\mathrm{i}\pi/3})| = \pi^{-1/2} (\rho^+ + 1/a)^{-1/2} \left(\frac{2\epsilon_+}{\rho^+ + 1/a}\right)^{-1/6}. \tag{3.9}$$

Then the matched new diffraction coefficient is given by

$$\alpha^{\mathrm{D}}_{A_1} = \frac{\pi^{1/2} (\rho^+ + 1/a)^{-1/3} \epsilon_+^{1/6}}{2^{5/6} r_0^{1/2}} \frac{1}{[\mathrm{Ai}'(-q_0)]^2 [1/N^2 - 1]}. \tag{3.10}$$

In **case II**, due to the diffracted waves, the creeping wave decays exponentially along the interface. (We remark that, if the interface is flat, the diffracted field is present only on the slow side, where it is called a "lateral wave" or "head wave". The corresponding wave then decays algebraically in distance s like $s^{-3/2}$.) Let ϵ_- denote the wavelength in the slow medium, and the wavelength in fast medium is defined by $\epsilon^+ = \frac{c^+}{c^-}\epsilon_-$.

For *tangentially diffracted wave*, the attenuation constant is

$$\beta_{A_3} = \beta_{A_2} = \frac{\sqrt{3}}{2} q_0 \left(\frac{\epsilon_+}{2}\right)^{-1/3} (\rho^+ + 1/a)^{2/3} - \frac{(\rho^+ + 1/a)}{\sqrt{1 - N^2}}. \tag{3.11}$$

For the *tangentially diffracted waves* outside the boundary layer in the fast medium, the diffraction coefficient is given by [8]

$$\alpha^{\mathrm{D}}_{A_2^{\mathrm{o}}} = \frac{\pi^{\frac{1}{3}}}{2^{\frac{1}{12}}} \left(\frac{\epsilon_+}{r}\right)^{\frac{1}{4}} [(\rho^+ + 1/a) r]^{-\frac{1}{2}} ((\rho^+ + 1/a)\epsilon_+)^{\frac{1}{6}} \frac{N[1 - N^2]^{-1/4}}{[\mathrm{Ai}'(-q_0)]^2 [1 - N^2]}. \tag{3.12}$$

While the diffraction coefficient $\alpha^{\mathrm{D}}_{A_2^{\mathrm{b}}}$ in the boundary layer is

$$\alpha^{\mathrm{D}}_{A_2^{\mathrm{b}}} = \frac{|\mathrm{Ai}[\frac{r}{\epsilon_+}(2\epsilon_+/a)^{\frac{1}{3}} \mathrm{e}^{-\mathrm{i}\pi/3}]|}{[\mathrm{Ai}'(-q_0)]^2 [1 - N^2]}.$$

The matched diffraction coefficient is given by

$$\alpha^{\mathrm{D}}_{A_2} = \frac{\pi^{\frac{1}{3}}}{2^{\frac{1}{12}}}\left(\frac{\epsilon_+}{r_0}\right)^{\frac{1}{4}}[(\rho^+ + 1/a)r_0]^{-\frac{1}{2}}((\rho^+ + 1/a)\epsilon_+)^{\frac{1}{6}}\frac{N[1-N^2]^{-1/4}}{[\mathrm{Ai}'(-q_0)]^2[1-N^2]} \tag{3.13}$$

with r_0 being the smallest positive r such that

$$\alpha^{\mathrm{D}}_{A_2^{\mathrm{o}}}(r) = \alpha^{\mathrm{D}}_{A_2^{\mathrm{b}}}(r).$$

For the *critically diffracted wave* in the slow medium, the diffraction coefficient outside the boundary layer is given by

$$\alpha^{\mathrm{D}}_{A_3^{\mathrm{o}}} = 2^{3/2}\left(\frac{\pi\epsilon_-}{r}\right)^{1/2}N(1-N^2)^{-1/2},$$

while in the boundary layer, the diffraction coefficient is

$$\alpha^{\mathrm{D}}_{A_3^{\mathrm{b}}} = \frac{|\mathrm{Ai}[(r/\epsilon_-)(2\epsilon_-/a)^{\frac{1}{3}}\mathrm{e}^{-\mathrm{i}\pi/3}]|}{\mathrm{Ai}(0)}.$$

Then the matched diffracted coefficient is

$$\alpha^{\mathrm{D}}_{A_3} = 2^{\frac{3}{2}}\left(\frac{\pi\epsilon_-}{r_0}\right)^{1/2}N(1-N^2)^{-1/2}, \tag{3.14}$$

with r_0 is the smallest positive number satisfies

$$\alpha^{\mathrm{D}}_{A_3^{\mathrm{o}}}(r) = \alpha^{\mathrm{D}}_{A_3^{\mathrm{b}}}(r).$$

Notice that for a flat interface, if $c(\mathbf{x}) \equiv C_1$ and $c(\mathbf{x}) \equiv C_2$, with C_1, C_2 constants on the two sides of the interface, respectively, then $\rho = 0, a^{-1} = 0$, so the diffraction coefficient vanishes. In this situation the diffraction term is not of order $\epsilon^{1/3}$, but of order ϵ, which is called "lateral wave" [3] and will be discussed in another paper.

3.2.2. *Type B interfaces*

For a **Type B** interface a diffracted wave can be produced by an incident wave in the following two ways (see Fig 2):

(I) When an incident wave on the slow medium hits the interface at the critical angle of incidence (like OB). It will produce a *reflected wave* (like BP_2), and a surface wave that travels along the fast side of the interface (like BCD), and continually sheds *critical diffracted waves* (DP_4) into the slow medium.

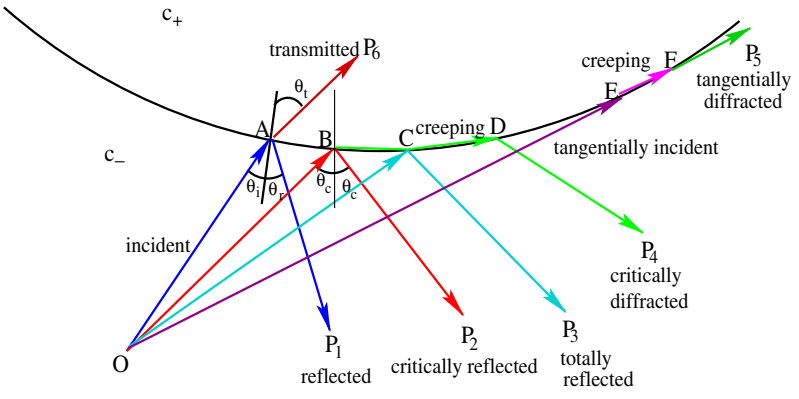

Fig. 2. Wave reflection, transmission and diffraction at a **Type B** interface.

(II) When an incident wave on the slow side hits the interface tangentially (like OF). A surface wave will propagate along the slow side of the interface (like EF), and continually sheds *tangentially diffracted waves* into the slow medium (like FP_5).

In **case I**, the attenuation constant of the *critically diffracted wave* in the slow medium is

$$\beta_{B_1} = \frac{\sqrt{3}}{2} q_0 (2\epsilon_-)^{-1/3} (\rho^- + 1/a)^{2/3} - \frac{\rho^- + 1/a}{\sqrt{1-N^2}}. \tag{3.15}$$

The matched diffraction coefficient in this case is

$$\alpha^{\mathrm{D}}_{B_1} = 2^{\frac{3}{2}} \left(\frac{\pi\epsilon_-}{r_0}\right)^{1/2} (1-N^2)^{-1/2} N, \tag{3.16}$$

where r_0 is the smallest positive solution of the following equation:

$$2^{\frac{3}{2}} \left(\frac{\epsilon_-\pi}{r}\right)^{1/2} (1-N^2)^{-1/2} N = \frac{|\mathrm{Ai}[(r/\epsilon_-)(2\epsilon_-/a)^{1/3} \mathrm{e}^{-\mathrm{i}\pi/3}]|}{\mathrm{Ai}(0)}.$$

In **case II**, for the *tangentially diffracted wave* in the slow medium, the attenuation constant is

$$\beta_{B_2} = \frac{\sqrt{3}}{2} q_0 (2\epsilon_-)^{-1/3} (\rho^- + 1/a)^{2/3} - \frac{\rho^- + 1/a}{\sqrt{1-N^2}}, \tag{3.17}$$

the matched diffraction coefficient is given by

$$\alpha^{\mathrm{D}}_{B_2} = \left(\frac{2\pi\epsilon_-}{r_0}\right)^{\frac{1}{2}} \left\{ \frac{(1-N^4)^{1/2} |\mathrm{Ai}'(q_0 \mathrm{e}^{\frac{2}{3}i\pi})|}{[(1-N^2)^{\frac{1}{2}} - N^2(1+N^2)^{\frac{1}{2}}] \mathrm{Ai}'(q_0)} - \left(\frac{a}{6\epsilon_-}\right)^{\frac{1}{3}} \frac{|\mathrm{Ai}(q_0 \mathrm{e}^{\frac{2}{3}i\pi})|}{\mathrm{Ai}'(q_0)} \right\} \tag{3.18}$$

with r_0 is the smallest positive solution of the following equation:

$$\left(\frac{2\pi\epsilon_-}{r}\right)^{\frac{1}{2}} \left\{ \frac{(1-N^4)^{1/2} |\mathrm{Ai}'(q_0 \mathrm{e}^{\frac{2}{3}i\pi})|}{[(1-N^2)^{\frac{1}{2}} - N^2(1+N^2)^{\frac{1}{2}}] \mathrm{Ai}'(q_0)} - \left(\frac{a}{6\epsilon_-}\right)^{\frac{1}{3}} \frac{|\mathrm{Ai}(q_0 \mathrm{e}^{\frac{2}{3}i\pi})|}{\mathrm{Ai}'(q_0)} \right\} = \left| \mathrm{Ai}\left[\epsilon_-^{-\frac{2}{3}} r \left(\frac{2}{a}\right)^{\frac{1}{3}} \mathrm{e}^{\frac{-i}{3}\pi} \right] \right|.$$

3.2.3. A summary on transmission, reflection and diffraction at a curved interface

We next discuss this behavior in more details when a plane incident wave hits a curved interface $\mathcal{C}$ (see Fig. 3).

Firstly, we parameterize the interface in terms of arclength s in the form

$$x = x(s), \quad y = y(s), \quad s_b \leqslant s \leqslant s_e. \tag{3.19}$$

We choose the arclength to increase with x (in a clockwise direction) and define the angle $\theta(s)$ to be the angle between the positive x-axis and the normal of a point on the interface.

This definition implies that the local normal $\mathbf{n}(s)$ and tangent $\mathbf{t}(s)$ are given directly by

$$\mathbf{n}(s) = (\cos\theta(s), \sin\theta(s)) \tag{3.20}$$

and

$$\mathbf{t}(s) = (-\sin\theta(s), \cos\theta(s)), \tag{3.21}$$

respectively. The radius of curvature $a(s)$ is given by

$$a(s) = \frac{1}{|\theta'(s)|} = \frac{1}{|x'y'' - x''y'|}. \tag{3.22}$$

Setting up a local coordinate system $(\mathbf{n}(s), \mathbf{t}(s))$ at the point of the interface, the original particle velocity $\mathbf{k} = (\xi, \eta)^t$ will become $\mathbf{k}' = (\xi', \eta')^t$ in this new coordinate system with $\mathbf{k}' = Q(s)\mathbf{k}$ where the rotation matrix $Q(s)$ is given by

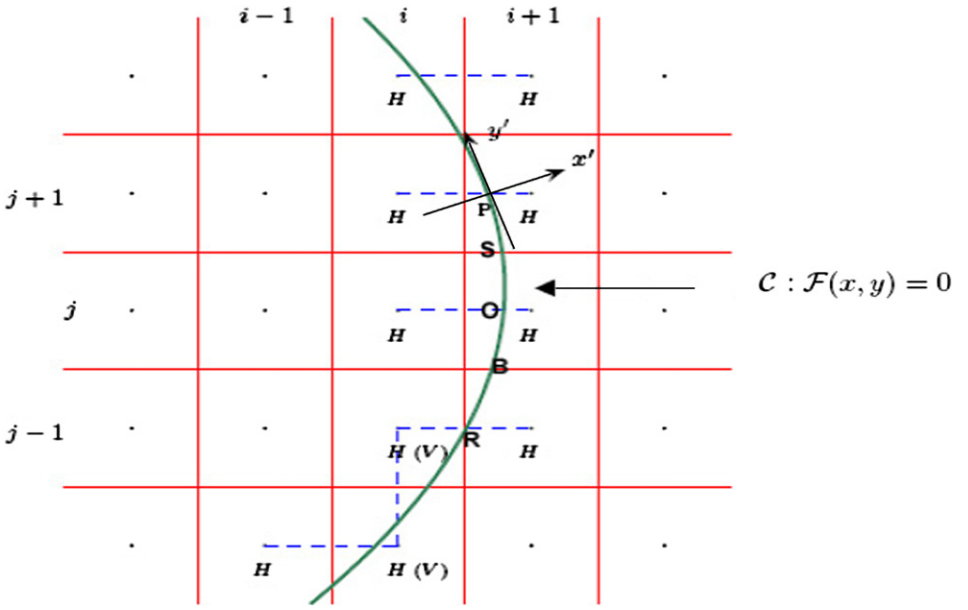

Fig. 3. Two-dimensional interface with irregular points labeled as 'H' and 'V'. The coordinates x' and y' are defined locally at the point P on the interface.

$$Q = \begin{pmatrix} \cos\theta(s) & \sin\theta(s) \\ -\sin\theta(s) & \cos\theta(s) \end{pmatrix}. \tag{3.23}$$

Then we can get the transmission and reflection $\alpha_{\pm}^{\mathrm{T}}, \alpha_{\pm}^{\mathrm{R}}$ for the incident wave hitting the interface in this local coordinate system by the way introduced in the following for a vertical interface, with axis $\mathbf{t}(s)$ as the interface. And for the corresponding velocity $\mathbf{k}'$ of the transmitted, reflected and diffracted waves, it can be obtained by applying the Hamiltonian preserving principle for $\mathbf{k}'$ in the local coordinate system and then transforming them back to the original system by multiplying $Q^{-1}(s)$. The new velocity obtained in this way still have a constant Hamiltonian in the original coordinate system because $Q(s)$ is an orthogonal matrix and $|\mathbf{k}'| = |\mathbf{k}|$.

We next discuss this behavior in more details when a plane incident wave hits interface $\mathcal{C}$ with a constant curvature. Again we will only discuss the case $c^+ > c^-$.

Let $\mathbf{x} = (x, y), \mathbf{k} = (\xi, \eta)^t$. Firstly, assume the incident wave with a velocity $\mathbf{k}_i = (\xi_i, \eta_i)^t$ hits the interface from the left, slow medium. We will use the Hamiltonian-preserving conditions locally in the direction normal to the interface as in [21].

In a local coordinate systems, (1.6) implies that η_i' is not changed i.e. $\eta_i' = \eta_t'$, when the wave crosses the interface, $\mathbf{k}_t = (\xi_t, \eta_t)^t$ is the velocity of transmitted wave. We introduce

$$\tau = \left(\frac{c^-}{c^+}\right)^2 (\xi_i')^2 + \left[\left(\frac{c^-}{c^+}\right)^2 - 1\right](\eta_i')^2 \tag{3.24}$$

which measures the criticality of wave transmission, reflection or diffraction.

If $\xi_i' > 0$, there are three possibilities:

- $\tau > 0$. Note this condition always holds when the wave propagates from the fast to the slow medium. In this case the wave can be partially transmitted and partially reflected. With reflection coefficient $\alpha_+^{\mathrm{R}} = \left(\frac{c^+\gamma_i - c^-\gamma_t}{c^+\gamma_i + c^-\gamma_t}\right)^2$ the wave is reflected with a new velocity $(\xi_r, \eta_r)^t = Q^{-1}(-\xi_i', \eta_i')^t$, where

$$\gamma_i = \frac{|\xi_i'|}{\sqrt{(\xi_i')^2 + (\eta_i')^2}}, \quad \gamma_t = \frac{|\xi_t'|}{\sqrt{(\xi_t')^2 + (\eta_t')^2}}$$

with transmission coefficient $\alpha_+^{\mathrm{T}} = 1 - \alpha_+^{\mathrm{R}}$ it will be transmitted with a new velocity $(\xi_t, \eta_t)^t = Q^{-1}(\xi_t', \eta_t')^t$, where

$$\xi_t' = \sqrt{\tau},$$

is obtained using (3.1).

- $\tau < 0$. In this case, there is no possibility for the wave to transmit, so the wave will be completely reflected with velocity (ξ_r, η_r).
- $\tau = 0$. This is the critical angle.
  1. For a **Type B** interface, there is no possibility for the wave to transmit into the fast medium, instead there is a partially reflected wave, and a surface wave along the surface of the fast medium, which decays with rate $e^{-\beta_{B_1} z}$, where z is the distance between the diffraction point and the incident point. The surface wave continuously sheds critically diffracted waves back into the slow media with diffraction coefficient $\alpha_{B_1,}^{\mathrm{D}}$.
  2. For a **Type A** interface, there is a partially reflected wave back to the slow medium, and a surface wave along the surface of the fast medium, which decays with rate $e^{-\beta_{A_2} z}$. The creeping wave sheds tangentially diffracted waves into the fast medium with diffraction coefficient $\alpha_{A_2}^{\mathrm{D}}$, and sheds critically diffracted waves into the slow medium with diffraction coefficient $\alpha_{A_3}^{\mathrm{D}}$.

If $\xi_i' = 0$, there are two other ways to generate diffracted waves:

- For a **Type B** interface, the incident wave will hit the interface tangentially and produce creeping waves propagating along the interface. As such a creeping wave travels along the interface, it continually sheds tangentially diffracted waves with diffraction coefficient $\alpha_{B_2}^{\mathrm{D}}$, and decays exponentially with a rate of $e^{-\beta_{B_2} z}$.
- For a **Type A** interface, the incident wave will hit the interface tangentially and produce creeping waves propagating along the interface. Part of the incident wave will transmit to the slow medium with transmission coefficient $1 - \alpha_{A_1}^{\mathrm{D}}$. As such a creeping wave travels along the interface, it continually sheds tangentially diffracted waves with diffraction coefficient $\alpha_{A_1}^{\mathrm{D}}$, and decay exponentially with a rate β_{A_1}.

If $\xi_i' < 0$, the behavior can be analyzed similarly with the reflection coefficient $\alpha_-^{\mathrm{R}} = \left(\frac{c^-\gamma_t - c^+\gamma_i}{c^-\gamma_t + c^+\gamma_i}\right)^2$, the transmission coefficient $\alpha_-^{\mathrm{T}} = 1 - \alpha_-^{\mathrm{R}}$, and the suitable attenuation constants and diffraction coefficients.

4. Interface conditions that account for transmission, reflection and diffraction

Usually, the solution of the Liouville equation (1.4), which is linearly hyperbolic, can be solved by the method of characteristics. When transmission and reflection both occur, f needs to be determined from two bicharacteristics, one accounting for the transmission and the other for reflection. This is how a unique solution to such a linear hyperbolic PDE with discontinuous and measure-valued coefficients is determined [24,26]. In order to capture the diffraction phenomena, the reflection and transmission terms must be supplemented with the diffraction term.

We will describe our method in the local coordinate system, and in the case of $c^+ > c^-$. Let

$$\tau = \left(\frac{c^-}{c^+}\right)^2 (\xi')^2 + \left[\left(\frac{c^-}{c^+}\right)^2 - 1\right](\eta')^2. \tag{4.1}$$

4.1. The *Type B* interface

We first discuss the **Type B** interface. For $\xi' > 0$, we use the following partial transmission and reflection condition at the interface:

$$f(t, \mathbf{x}^+, \xi', \eta') = \alpha_+^{\mathrm{T}} f(t, \mathbf{x}^-, \xi_t', \eta_t') + \alpha_+^{\mathrm{R}} f(t, \mathbf{x}^+, -\xi', \eta'), \quad \xi_t' > 0 \tag{4.2}$$

with $\eta_t' = \eta'$ and ξ_t' obtained from $\xi\prime$ through the constant condition (1.5).

For $\xi' < 0$, there are three possibilities:

1. if $\tau > 0$ (partial reflection and transmission), then
$$f(t,\mathbf{x}^-,\xi',\eta') = \alpha_-^{\mathrm{R}} f(t,\mathbf{x}^-,-\xi',\eta') + \alpha_-^{\mathrm{T}} f(t,\mathbf{x}^+,\xi_t',\eta_t'). \tag{4.3}$$
2. if $\tau < 0$ (complete reflection), the interface condition is
$$f(t,\mathbf{x}^-,\xi',\eta') = f(t,\mathbf{x}^-,-\xi',\eta'). \tag{4.4}$$
3. if $\tau = 0$ (**case I**), there will be some diffractions, so the interface condition is
$$\begin{aligned} f(t,\mathbf{x}^-(s),\xi',\eta') = {} & \alpha_{B_1}^{\mathrm{D}}(\mathbf{x}(s)) \int_{s_b}^{s} \alpha_{B_1}^{\mathrm{D}}(\mathbf{x}(s_q)) \mathrm{e}^{-\int_{s_q}^{s} \beta_{B_1}(\mathbf{x}(z))\mathrm{d}z} \cdot \int_{\Gamma_q} f(t-\bar{t}_q,\mathbf{x}^-(s_q),\xi_q',\eta'(\xi_q'))\mathrm{d}\xi_q'\,\mathrm{d}s_q \\ & + (1-\alpha_{B_1}^{\mathrm{D}}(\mathbf{x}(s)))f(t,\mathbf{x}^-(s),-\xi',\eta'), \end{aligned} \tag{4.5}$$

here Γ_q is the *line of critical angle*

$$\frac{\xi_q'}{\eta_q'} = \mathrm{sgn}(\eta')\sqrt{\left(\frac{c^+(\mathbf{x}(s_q))}{c^-(\mathbf{x}(s_q))}\right)^2 - 1}. \tag{4.6}$$

In (4.5), the first term is the critically diffracted wave into the slow medium that was originated from the incident critical wave from the slow medium, $\bar{t}_q = |\int_{s_q}^{s} \frac{\mathrm{d}z}{c^+(\mathbf{x}(z))}|$ is the average propagation time between the incident point $\mathbf{x}(s_q)$ and the diffracted point $\mathbf{x}(s)$, and $(\mathbf{x}^-(s_q),\xi_q',\eta'(\xi_q'))$ are the points and critical angles at which the surface waves are generated. The second term in (4.5) is the critically reflected wave by the incident critical wave from the slow medium, where $1-\alpha_{B_1}^{\mathrm{D}}(\mathbf{x}(s))$ is the reflection coefficient at critical angle, in this case part of the waves at this point will become surface waves in the faster medium and diffract into other points, so $1-\alpha_{B_1}^{\mathrm{D}}(\mathbf{x}(s))$ is derived by the fact that the reflection term is the difference between the incident wave and the creeping wave generated from this point.

For notation simplicity, below we will use $\mathbf{x}$ to denote $\mathbf{x}(s)$ and $\mathbf{x}_q$ to denote $\mathbf{x}(s_q)$.

If $\xi' = 0$ (**case II**), there will be some tangentially diffracted waves, so

$$\begin{aligned} f(t,\mathbf{x}^-,\xi',\eta') = {} & \alpha_{B_2}^{\mathrm{D}}(\mathbf{x}) \int_{s_b}^{s} \alpha_{B_2}^{\mathrm{D}}(\mathbf{x}_q) \mathrm{e}^{-\int_{s_q}^{s} \beta_{B_2}(\mathbf{x}(z))\mathrm{d}z} \mathrm{sgn}(\eta') \int_0^{\mathrm{sgn}(\eta')\infty} f_-(t-\bar{t}_q,\mathbf{x}_q^-,0,\eta_q')\mathrm{d}\eta_q'\,\mathrm{d}s \\ & + (1-\alpha_{B_2}^{\mathrm{D}}(\mathbf{x}))f_-(t,\mathbf{x}^-,\xi',\eta'), \end{aligned} \tag{4.7}$$

where $\bar{t}_q = |\int_{s_q}^{s} \frac{\mathrm{d}z}{c^-(z)}|$ is the average time,

$$f_-(t,\mathbf{x},\xi',\eta') = \lim_{\omega\to 0^+} f(t,\mathbf{x}-\omega\mathbf{k}',\xi',\eta').$$

In this case, the incident wave tangentially hits the interface from the slow side. Part of the incident wave transforms into the creeping wave with coefficient $\alpha_{B_2}^{\mathrm{D}}$, and part of the incident wave travels through tangentially with coefficient $1-\alpha_{B_2}^{\mathrm{D}}$.

4.2. The *Type A* interface

Next, we consider a **Type A** interface. For $\xi' > 0$, it is still the following partial transmission and reflection condition:

$$f(t,\mathbf{x}^+,\xi',\eta') = \alpha_+^{\mathrm{T}} f(t,\mathbf{x}^-,\xi_t',\eta_t') + \alpha_+^{\mathrm{R}} f(t,\mathbf{x}^+,-\xi',\eta'), \quad \xi_t' > 0. \tag{4.8}$$

If $\xi' < 0$, there are three possibilities.

1. if $\tau > 0$ (partial reflection and transmission), then
$$f(t,\mathbf{x}^-,\xi',\eta') = \alpha_-^{\mathrm{R}} f(t,\mathbf{x}^-,-\xi',\eta') + \alpha_-^{\mathrm{T}} f(t,\mathbf{x}^+,\xi_t',\eta_t'). \tag{4.9}$$

2. if $\tau < 0$ (complete reflection), the interface condition is

$$f(t,\mathbf{x}^-,\xi',\eta') = f(t,\mathbf{x}^-,-\xi',\eta'). \tag{4.10}$$

3. if $\tau = 0$ (**case II**), there will be some diffractions, so the interface condition is

$$\begin{aligned} f(t,\mathbf{x}^-,\xi',\eta') &= \alpha^{\mathrm{D}}_{A_3}(\mathbf{x})\int_{s_b}^{s}\alpha^{\mathrm{D}}_{A_3}(\mathbf{x}_q)\mathrm{e}^{-\int_{s_q}^{s}\beta_{A_3}(\mathbf{x}(z))\mathrm{d}z}\int_{\Gamma_q} f(t-\bar{t}_q,\mathbf{x}_q^-,\xi'_q,\eta'_q(\xi'_q))d\xi'_q\,\mathrm{d}s \\ &\quad + (1-\alpha^{\mathrm{D}}_{A_1}(\mathbf{x}))\int_{s_b}^{s}\alpha^{\mathrm{D}}_{A_1}(\mathbf{x}_q)\mathrm{e}^{-\int_{s_q}^{s}\beta_{A_1}(\mathbf{x}(z))\mathrm{d}z}\mathrm{sgn}(\eta'_q)\int_0^{+\infty\,\mathrm{sgn}(\eta'_q)} f_-(t-\bar{t}_q,\mathbf{x}_q^+,0,\eta'_q)\mathrm{d}\eta'_q\,\mathrm{d}s, \\ &\quad + \left(1-\alpha^{\mathrm{D}}_{A_3}(\mathbf{x})\right)f(t,\mathbf{x}^-,-\xi',\eta'). \end{aligned} \tag{4.11}$$

In (4.11), the first term represents the critically diffracted wave into the slow medium that was originated from the critical incident wave from the slow medium, the second term represents the critically transmitted wave into the slow medium that was originated from the tangential incident wave from the fast medium, while the third term represents the critically reflected wave into the slow medium that was originated from the critical incident wave from the slow medium.

For $\xi' = 0$ (**case I**),

$$\begin{aligned} f(t,\mathbf{x}^+,\xi',\eta') &= \alpha^{\mathrm{D}}_{A_1}(\mathbf{x})\int_{s_b}^{s}\alpha^{\mathrm{D}}_{A_1}(\mathbf{x}_q)\mathrm{e}^{-\int_{s_q}^{s}\beta_{A_1}(\mathbf{x}(z))\mathrm{d}z}\mathrm{sgn}(\eta'_q)\int_0^{+\infty\,\mathrm{sgn}(\eta'_q)} f_-(t-\bar{t}_q,\mathbf{x}_q^+,0,\eta'_q)\mathrm{d}\eta'_q\,\mathrm{d}s \\ &\quad + \alpha^{\mathrm{D}}_{A_2}(\mathbf{x})\int_{s_b}^{s}\alpha^{\mathrm{D}}_{A_2}(\mathbf{x}_q)\mathrm{e}^{-\int_{s_q}^{s}\beta_{A_2}(\mathbf{x}(z))\mathrm{d}z}\int_{\Gamma_q} f(t-\bar{t}_q,\mathbf{x}_q^-,\xi'_q,\eta'_q(\xi'_q))\mathrm{d}\xi'_q\,\mathrm{d}s. \end{aligned} \tag{4.12}$$

In (4.12), the first term represents the tangentially diffracted wave originated from the tangentially incident wave from the fast medium, while the second term represents the tangentially diffractive wave originated from the critically incident wave from the slow medium. When $\xi' = 0$ the wave hits the interface tangentially from the fast side of the interface and produces the tangentially diffracted waves with diffraction coefficient $\alpha^{\mathrm{D}}_{A_1}$ and the critically transmitted waves with transmission coefficient $1-\alpha^{\mathrm{D}}_{A_1}$. The velocities in Γ_q satisfy $\left(\frac{c^-}{c^+}\right)^2(\xi'_q)^2 + \left[\left(\frac{c^-}{c^+}\right)^2 - 1\right](\eta'_q)^2 = 0$.

After getting the interface condition in the local coordinates systems, we use $\mathbf{k} = (\xi,\eta)^t = Q^{-1}\mathbf{k}' = Q^{-1}(\xi',\eta')^t$ to get the interface condition in the original coordinate systems.

The case $c^- > c^+$ can be similarly considered, since in this case one just needs to interchange the **Type A** with the **Type B** interfaces.

The interface condition (4.2)–(4.12) is the main idea in this paper, and will be used in constructing the numerical flux across the interface in our paper.

5. The numerical scheme

5.1. The numerical flux

Consider the 2D Liouville equation

$$f_t + \frac{c(x,y)\xi}{\sqrt{\xi^2+\eta^2}}f_x + \frac{c(x,y)\eta}{\sqrt{\xi^2+\eta^2}}f_y - c_x\sqrt{\xi^2+\eta^2}f_\xi - c_y\sqrt{\xi^2+\eta^2}f_\eta = 0. \tag{5.1}$$

Without loss of generality, we employ a uniform mesh with grid points at $x_{i+\frac{1}{2}},\ i=0,\ldots,M$ in the x direction, $y_{j+\frac{1}{2}},\ j=0,\ldots,N$ in the y direction, $\xi_{k+\frac{1}{2}},\ k=0,\ldots,K$ in the ξ direction and $\eta_{l+\frac{1}{2}},\ l=0,\ldots,L$ in the η direction. The cells are centered at (x_i,y_j,ξ_k,η_l) with $x_i = \frac{1}{2}\left(x_{i-\frac{1}{2}}+x_{i+\frac{1}{2}}\right),\ y_j = \frac{1}{2}\left(y_{j-\frac{1}{2}}+y_{j+\frac{1}{2}}\right),\ \xi_k = \frac{1}{2}\left(\xi_{k-\frac{1}{2}}+\xi_{k+\frac{1}{2}}\right),$ $\eta_l = \frac{1}{2}\left(\eta_{l-\frac{1}{2}}+\eta_{l+\frac{1}{2}}\right)$. The mesh sizes are denoted by $\Delta x = x_{i+\frac{1}{2}} - x_{i-\frac{1}{2}},\ \Delta y = y_{j+\frac{1}{2}} - y_{j-\frac{1}{2}},\ \Delta\xi = \xi_{k+\frac{1}{2}} - \xi_{k-\frac{1}{2}},$ $\Delta\eta = \eta_{l+\frac{1}{2}} - \eta_{l-\frac{1}{2}}$. Let Δt be the time step, $t^n = n\Delta t$. The cell average of f is defined as

$$f_{ijkl} = \frac{1}{\Delta x \Delta y \Delta \xi \Delta \eta} \int_{x_{i-\frac{1}{2}}}^{x_{i+\frac{1}{2}}} \int_{y_{j-\frac{1}{2}}}^{y_{j+\frac{1}{2}}} \int_{\xi_{k-\frac{1}{2}}}^{\xi_{k+\frac{1}{2}}} \int_{\eta_{l-\frac{1}{2}}}^{\eta_{l+\frac{1}{2}}} f(x,y,\xi,\eta) \mathrm{d}\eta \, \mathrm{d}\xi \, \mathrm{d}y \, \mathrm{d}x, \tag{5.2}$$

while $f^n_{ijkl} = f_{ijkl}(t^n)$.

We approximate $c(x,y)$ by a piecewise bilinear function, and always provide two interface values of $c(x,y)$ at each cell interface. Let the cell interface value of $c(x,y)$ be $c^{\pm}_{i\pm 1/2,j} = \frac{1}{\Delta y} \int_{y_{j-1/2}}^{y_{j+1/2}} c(x^{\pm}_{i\pm 1/2}, y) \mathrm{d}y$, and $c^{\pm}_{i,j\pm 1/2}$ defined similarly. When $c(x,y)$ is smooth at a cell interface, the two interface values are identical. We also define the average wave speed in a cell by averaging the four cell interface values

$$c_{ij} = \frac{1}{4}(c^+_{i-\frac{1}{2},j} + c^-_{i+\frac{1}{2},j} + c^+_{i,j-\frac{1}{2}} + c^-_{i,j+\frac{1}{2}}).$$

The 2D Liouville equation (5.1) can be semi-discretized as

$$\begin{aligned}
&(f_{ijkl})_t + \frac{c_{ij}\xi_k}{\Delta x \sqrt{\xi_k^2 + \eta_l^2}} \left(f_{i+\frac{1}{2},jkl} - f^+_{i-\frac{1}{2},jkl} \right) + \frac{c_{ij}\eta_l}{\Delta y \sqrt{\xi_k^2 + \eta_l^2}} \left(f_{i,j+\frac{1}{2},kl} - f^+_{i,j-\frac{1}{2},kl} \right) \\
&- \frac{c_{i+\frac{1}{2},j} - c^+_{i-\frac{1}{2},j}}{\Delta x \Delta \xi} \sqrt{\xi_k^2 + \eta_l^2} \left(f_{ij,k+\frac{1}{2},l} - f_{ij,k-\frac{1}{2},l} \right) - \frac{c_{i,j+\frac{1}{2}} - c^+_{i,j-\frac{1}{2}}}{\Delta y \Delta \eta} \sqrt{\xi_k^2 + \eta_l^2} \left(f_{ijk,l+\frac{1}{2}} - f_{ijk,l-\frac{1}{2}} \right) = 0,
\end{aligned}$$

where the numerical fluxes $f_{ij,k+\frac{1}{2},l}$ and $f_{ijk,l+\frac{1}{2}}$ are defined using the upwind discretization. The essential part of our algorithm is to define the splitting numerical fluxes $f^{\pm}_{i+\frac{1}{2},jkl}$, $f^{\pm}_{i,j+\frac{1}{2},kj}$ at each cell interface. We will use the interface conditions (4.2)–(4.12) to construct these fluxes.

Assume $c(x,y)$ is discontinuous at $x_{i+\frac{1}{2}}$, and $c^-_{i+1/2,j} < c^+_{i+1/2,j}$. Consider the case $\xi'_k > 0$. The upwind scheme yields $f^-_{i+\frac{1}{2},jkl} = f_{ijkl}$ and the interface condition (4.2) gives

$$f^+_{i+\frac{1}{2},jkl} = \alpha^{\mathrm{T}}_+ f(t, x_i, y_j, \xi_t, \eta_t) + \alpha^{\mathrm{R}}_+ f(t, x_{i+1}, y_j, \xi_r, \eta_r), \tag{5.3}$$

where $(\xi,\eta)^t = Q^{-1}(\xi',\eta')^t$, $(\xi_r,\eta_r)^t = Q^{-1}(-\xi'_k,\eta'_l)^t$, and ξ'_t is obtained from using $\eta'_l = \eta'_l$ in (3.1) with (ξ',η') in local coordinate systems. Then transform this interface condition into the original coordinate system (ξ,η). Since $(\xi_t,\eta_t), (\xi_r,\eta_r)$ may not be grid points, we have to define them approximately. One can first locate the cell centers that bound these velocities, and then use a bilinear interpolation to evaluate the needed numerical flux at (ξ_t,η_t) or (ξ_r,η_r).

The case $\xi'_k < 0$ depends on the specific type of the interface, which we discuss below in details.

5.1.1. The *Type B* interface

First, $f^+_{i+\frac{1}{2},jkl} = f_{i+1,jkl}$ by the upwind scheme. Let

$$\tau_{i+1/2,j} = \left(\frac{c^-_{i+1/2,j}}{c^+_{i+1/2,j}} \right)^2 (\xi'_k)^2 + \left[\left(\frac{c^-_{i+1/2,j}}{c^+_{i+1/2,j}} \right)^2 - 1 \right] (\eta'_l)^2. \tag{5.4}$$

We define the numerical flux according to the interface conditions (4.3)–(4.5).

1. If $\tau_{i+1/2,j} > 0$, then

$$f^-_{i+\frac{1}{2},jkl} = \alpha^{\mathrm{R}}_- f(t, x_i, y_j, \xi_r, \eta_r) + \alpha^{\mathrm{T}}_- f(t, x_{i+1}, y_j, \xi_t, \eta_t), \tag{5.5}$$

   where $(\xi,\eta)^t = Q^{-1}(\xi',\eta')^t$, $(\xi_r,\eta_r)^t = Q^{-1}(-\xi'_k,\eta'_l)^t$, and ξ'_t is obtained from (3.1) by setting $\eta'_l = \eta'_t$.
2. If $\tau_{i+1/2,j} < 0$, then

$$f^-_{i+\frac{1}{2},jkl} = f(t, x_i, y_j, \xi_r, \eta_r). \tag{5.6}$$

3. If $\tau_{i+1/2,j} = 0$, then we discretize the arclength s of the interface with $s_q, q = 0, 1, \ldots, O$. Assume that $(x_{i+\frac{1}{2}}, y_j) = (x(s_p), y(s_p))$ and denote $f(t, x_{i_q}, y_{j_q}, \xi, \eta)$ by $f(\mathbf{x}(s_q), \xi, \eta)$. By approximating (4.5) (we only write the case of $\xi'_k > 0$, the case of $\xi'_k < 0$ is similar):

$$f^-_{i+\frac{1}{2},jkl}(t) = \alpha^{\mathrm{D}}_{B_1}(\mathbf{x}(s_p)) \sum_{q=0}^{p} \left[\alpha^{\mathrm{D}}_{B_1}(\mathbf{x}(s_q)) \mathrm{e}^{-\sum_{j'=0}^{q} \beta_{B_1}(\mathbf{x}(s_{j'}))\Delta s} \sum_{m=0}^{K} f\big(t-\bar{t}_q, \mathbf{x}(s_q), \xi_m, \eta(\xi_m)\big)\Delta s \Delta\xi \right] + \Big(1-\alpha^{\mathrm{D}}_{B_1}(\mathbf{x}(s_p))\Big) f(t, x_i, y_j, \xi_r, \eta_r) \tag{5.7}$$

with $\bar{t}_q = \sum_{j'=j_q}^{j} \frac{\Delta s}{c^+(s_{j'})}$, and $c^+(s_{j'}) = c^+(x(s_{j'}), y(s_{j'}))$. The critical angles $(\xi'_m, \eta'(\xi_m))$ in the local coordinate system satisfy $\left(\frac{c^-(s_q)}{c^+(s_q)}\right)^2 (\xi'_m)^2 + \left[\left(\frac{c^-(s_q)}{c^+(s_q)}\right)^2 - 1\right](\eta'(\xi'_m))^2 = 0$. Since $t^n - \bar{t}_q$ may not be a grid point in the time direction, we have to define it approximately. One can first locate the two adjacent discrete time, and then use a linear interpolation to evaluate the needed numerical density at time $t^n - \bar{t}_q$. In practical computation, we need to save the numerical flux at the interface for the previous time steps.

If $\xi'_k = 0$ (**case II**, tangent incidence and diffraction), then according to (4.7),

$$f^-_{i+\frac{1}{2},jkl}(t) = \alpha^{\mathrm{D}}_{B_2}(\mathbf{x}(s_p)) \sum_{q=0}^{p} \left[\alpha^{\mathrm{D}}_{B_2}(\mathbf{x}(s_q)) \mathrm{e}^{-\sum_{j'=0}^{q} \beta_{B_2,}(\mathbf{x}(s_{j'}))\Delta s} \sum_{c=0}^{L} f_-(t-\bar{t}_q, \mathbf{x}(s_q), \xi_m, \eta_c) \right] \Delta s \Delta\eta + \Big(1-\alpha^{\mathrm{D}}_{B_2}(\mathbf{x}(s_p))\Big) f(t, x_i, y_j, \xi_r, \eta_r) \tag{5.8}$$

with $\xi'_m = 0$.

*5.1.2. The **Type A** interface*

If $\xi'_k < 0$ and for non-critical angles, the numerical flux $f^-_{i+\frac{1}{2},jkl}$ is defined by (5.5). The difference lies in the case when the wave hits the interface with the critical or tangent angle of incidence, namely, $\tau_{i+1/2,j} = 0$ or $\xi'_k = 0$.

For a critical angle, by approximating (4.11), we obtain (for the case of $\eta' > 0$),

$$f^-_{i+\frac{1}{2},jkl}(t) = \alpha^{\mathrm{D}}_{A_3}(\mathbf{x}(s_p)) \sum_{q=0}^{p} \left[\alpha^{\mathrm{D}}_{A_3}(x(s_q)) \mathrm{e}^{-\sum_{j'=0}^{q} \beta_{A_3}(\mathbf{x}(s_{j'}))\Delta s} \sum_{m=0}^{K} f(t-\bar{t}_q, \mathbf{x}(s_q), \xi_m, \eta(\xi_m))\Delta s \Delta\xi \right] + (1-\alpha^{\mathrm{D}}_{A_1}(\mathbf{x}(s_p))) \sum_{q=0}^{p} \left[\alpha^{\mathrm{D}}_{A_1}(\mathbf{x}(s_q)) \mathrm{e}^{-\sum_{j'=0}^{q} \beta_{A_1}(\mathbf{x}(s_{j'}))\Delta s} \sum_{c=0}^{L} f(t-\bar{t}_{q_1}, \mathbf{x}(s_q), \xi_{k_m}, \eta_c)\Delta s \Delta\eta \right] + \Big(1-\alpha^{\mathrm{D}}_{A_3}(\mathbf{x}(s_p))\Big) f(t, x_i, y_j, \xi_r, \eta_r) \tag{5.9}$$

with critical angles $(\xi'_m, \eta'(\xi'_m))$ satisfying $\left(\frac{c^-(s_q)}{c^+(s_q)}\right)^2 (\xi'_m)^2 + \left[\left(\frac{c^-(s_q)}{c^+(s_q)}\right)^2 - 1\right](\eta'(\xi'_m))^2 = 0$, and $\xi'_{k_m} = 0$ are the velocities of the waves in the local coordinate, which hit the interface tangentially from the fast side of the interface and produces the tangentially diffracted waves and critically transmitted waves.

If $\xi'_k = 0$ (**case I**, tangent incidence and diffraction), using interface condition (4.12), we have

$$f^+_{i+\frac{1}{2},jkl}(t) = \alpha^{\mathrm{D}}_{A_1}(\mathbf{x}(s_p)) \sum_{q=0}^{p} \left[\alpha^{\mathrm{D}}_{A_1}(\mathbf{x}(s_q)) \mathrm{e}^{-\sum_{j'=0}^{q} \beta_{A_1}(\mathbf{x}(s_{j'}))\Delta s} \sum_{c=0}^{L} f_-(t-\bar{t}_{q_1}, \mathbf{x}(s_q), \xi_{k_m}, \eta_c)\Delta s \Delta\eta \right] + \alpha^{\mathrm{D}}_{A_2}(\mathbf{x}(s_p)) \sum_{q=0}^{p} \left[\alpha^{\mathrm{D}}_{A_2}(\mathbf{x}(s_q)) \mathrm{e}^{-\sum_{j'=0}^{q} \beta_{A_2}(\mathbf{x}(s_{j'}))\Delta s} \sum_{m=0}^{K} f(t-\bar{t}_q, \mathbf{x}(s_q), \xi_m, \eta(\xi_m))\Delta s \Delta\xi \right], \tag{5.10}$$

with $\xi'_{k_m} = 0$ and $(\xi'_m, \eta'(\xi'_m))$ satisfy $\left(\frac{c^-}{c^+}\right)^2(\xi'_m)^2 + \left[\left(\frac{c^-}{c^+}\right)^2 - 1\right](\eta'(\xi'_m))^2 = 0$, where the waves hit the interface from the slow media with a critical incident angle and produces the critically transmitted wave along the fast side of the interface, which sheds diffracted waves at every point they passes by.

In the case $\xi'_k > 0$ and $c^-_{i+1/2,j} > c^+_{i+1/2,j}$, $f^+_{i+1/2,jkl}$ can be similarly defined for diffraction.

In practical computations, we compute the critical angle by solving $\frac{\xi'}{\eta'} = \pm\sqrt{\left(\frac{c^+}{c^-}\right)^2 - 1}$ at the interface. Since we cannot get $\xi' = 0$ numerically, we use the condition $|\xi'| < \sigma$, with the constant σ sufficiently small (say about the mesh size) as the numerical zero, as the condition for tangent angle. In our experiments, when $\sigma < 10^{-5}$, the choice of σ does not affect the numerical results.

5.2. Approximation along the curved interface

Before discussing the detailed algorithm, let us show how to calculate the quantity along the curved interface. Suppose we have an interface given by a curve $\mathcal{C}$, defined by the equation

$$\mathcal{F}_{\text{int}}(x, y) = 0.$$

We classify the grid points into the following categories (see Fig. 2), as done in [21]:

1. Sweep along the horizontal direction for each j and flag the points adjacent to the interface from the right and the left. These points are called horizontal irregular points and labeled with 'H'.
2. Sweep along the vertical direction for each i and flag the points which are adjacent to the interface from the top and the bottom. These points are called vertical irregular points and labeled with 'V'.
3. All the other points are regular points.

After we determine the irregular points, the cell interface between two horizontally adjacent irregular points and also two vertically adjacent irregular points can be seen as an approximation to the real interface curve $\mathcal{C}$. By doing this, we can still assign our averaged wave speed as what we introduce in Section 4.1.

Connecting these two points by a dashed line as in the figure and it must have an intersection with the interface, say P.

The exponential decaying term is evaluated by the following method. The decay factor between the point P and O is defined by $\exp\{-\beta_+(S)r_{PO}\}$ with S is the point of intersection of mesh line along $y_{j+1/2}$ and the interface, and $r_{PO} = \sqrt{(x_P - x_O)^2 + (y_P - y_O)^2}$ is the distance between P, O. Similarly, $\bar{t}_q$ between P and O is defined by $r_{PO}/c^+(S)$, here $c^+(S)$ is the wave speed at point S. The decay rate between the point P and R is defined by $\exp\{-\beta_+(S)r_{PO} - \beta_+(B)r_{OR}\}$ and the time $\bar{t}_q$ is $r_{PO}/c^+(S) + r_{OR}/c^+(B)$.

After getting the coefficients, decay rates and corresponding velocities, we can calculate the splitting numerical fluxes $f^{\pm}_{i+1/2,jkl}$ and $f^{\pm}_{i,j+1/2,kl}$ by the algorithm in this section. Here effectively we moved P to the nearest mesh point, resulting an $O(\Delta x, \Delta y)$ error. The above techniques can be applied for any interface curve as long as there is an explicit expression for it.

The detailed algorithm to generate the numerical flux at $t = t^n$ is given in the Appendix.

In order to capture the effect of the diffractions, *only* near the interface the mesh size must be the same order of the diffracted coefficients (in the numerical examples given in this paper, this means $\Delta x, \Delta y \Delta\xi, \Delta\eta \sim O(\epsilon^{\frac{1}{3}})$). This means that the computational cost will be more than the Hamiltonian preserving scheme in [26] that captures only transmissions and reflections.

5.3. Positivity of the numerical scheme

Now we consider the finite difference approach. For simplicity, we only consider the forward Euler scheme in time. Without loss of generality, we consider the case $\xi_k < 0, \eta_l > 0$ and $c^-_{i+\frac{1}{2},j} \geqslant c^+_{i-\frac{1}{2},j}$ for all i, $c^-_{i,j+\frac{1}{2}} \leqslant c^+_{i,j-\frac{1}{2}}$ for all j and the point $x_{i+\frac{1}{2}}, y_j$ is on the **Type B** interface.

First, for non-critical angles, the scheme is same as the scheme in [26].

For critical angles, the scheme reads:

$$\frac{f_{ijkl}^{n+1}-f_{ijkl}^{n}}{\Delta t}=\frac{c_{ij}\gamma_t}{\Delta x}\left[\alpha_{B_{1,-}}^{\mathrm{D}}\sum_{q,m}\alpha_{B_{1,-}}^{\mathrm{D}}\mathrm{e}^{-\sum_{j'=j_q}^{j_p}\beta_{B_{1,-}}(j')\sqrt{\Delta y^2+\Delta x^2}}\Delta y\Delta\xi\left(d_1 f_{i_q,j_q,k_m,l_m}^{n_q}+d_2 f_{i_q,j_q,k_m,l_m}^{n_q+1}\right)\right.$$
$$\left.+\left(1-\alpha_{B_{1,-}}^{\mathrm{D}}\right)\left(b_1 f_{i,j,k_1+1,l_1+1}^{n}+b_2 f_{i,j,k_1,l_1+1}^{n}+b_3 f_{i,j,k_1,l_1}^{n}+b_4 f_{i,j,k_1+1,l_1}^{n}\right)-f_{ijkl}^{n}\right]$$
$$-\frac{c_{ij}\gamma_i}{\Delta y}\left(f_{ijkl}^{n}-f_{i,j-1,kl}^{n}\right)+\frac{\left(c_{i+\frac{1}{2},j}-c_{i-\frac{1}{2},j}^{+}\right)}{\Delta x\Delta\xi}\sqrt{\xi_k^2+\eta_l^2}\left(f_{ij,k+1,l}^{n}-f_{ijkl}^{n}\right)$$
$$+\frac{\left(c_{i,j+\frac{1}{2}}-c_{i,j-\frac{1}{2}}^{+}\right)}{\Delta y\Delta\eta}\sqrt{\xi_k^2+\eta_l^2}\left(f_{ijkl}^{n}-f_{ijk,l-1}^{n}\right),$$

where $d_1+d_2=1, b_1+b_2+b_3+b_4=1$ are nonnegative numbers.

Namely,

$$f_{ijkl}^{n+1}=\left[1-c_{ij}\lambda_x^t\gamma_t-c_{ij}\lambda_y^t\gamma_i-\frac{|c_{i+\frac{1}{2},j}-c_{i-\frac{1}{2},j}^{+}|}{\Delta x}\lambda_\xi^t\sqrt{\xi_k^2+\eta_l^2}-\frac{\left|c_{i,j+\frac{1}{2}}-c_{i,j-\frac{1}{2}}^{+}\right|}{\Delta y}\lambda_\eta^t\sqrt{\xi_k^2+\eta_l^2}\right]f_{ijkl}^{n}$$
$$+\frac{\left|c_{i+\frac{1}{2},j}^{-}-c_{i-\frac{1}{2},j}^{+}\right|}{\Delta x}\lambda_\xi^t\sqrt{\xi_k^2+\eta_l^2}f_{ij,k+1,l}^{n}$$
$$+c_{ij}\lambda_x^t\gamma_t\alpha_{B_{1,-}}^{\mathrm{D}}\sum_{q,m}\alpha_{B_{1,-}}^{\mathrm{D}}\mathrm{e}^{-\sum_{j'=j_q}^{j_p}\beta_{B_{1,-}}(j')\sqrt{\Delta x^2+\Delta y^2}}\left(d_1 f_{i_q,j_q,k_m,l_m}^{n_q}+d_2 f_{i_q,j_q,k_m,l_m}^{n_q+1}\right)\Delta y\Delta\xi$$
$$+c_{ij}\gamma_t\lambda_x^t\left(1-\alpha_{B_{1,-}}^{\mathrm{D}}\right)\left(b_1 f_{i,j,k_1+1,l_1+1}^{n}+b_2 f_{i,j,k_1,l_1+1}^{n}+b_3 f_{i,j,k_1,l_1}^{n}+b_4 f_{i,j,k_1+1,l_1}^{n}\right)$$
$$+c_{ij}\lambda_y^t\gamma_i f_{i,j-1,kl}^{n}+\frac{\left|c_{i,j+\frac{1}{2}}-c_{i,j-\frac{1}{2}}^{+}\right|}{\Delta y}\lambda_\eta^t\sqrt{\xi_k^2+\eta_l^2}f_{ijk,l-1}^{n},\tag{5.11}$$

where $\lambda_x^t=\frac{\Delta t}{\Delta x},\lambda_y^t=\frac{\Delta t}{\Delta y},\lambda_\xi^t=\frac{\Delta t}{\Delta\xi},\lambda_\eta^t=\frac{\Delta t}{\Delta\eta}$.

Now we investigate the positivity of scheme (5.11). This is to prove that if $f_{ijkl}^{n}\geqslant 0$ for all (i,j,k,l), then this is also true for f_{ijkl}^{n+1}. Clearly one just needs to show that all the coefficients before f^n are non-negative. A sufficient condition for this is clearly

$$1-c_{ij}\gamma_t\lambda_x^t-c_{ij}\gamma_i\lambda_y^t-\left(\frac{\left|c_{i+\frac{1}{2},j}-c_{i-\frac{1}{2},j}^{+}\right|}{\Delta x}\lambda_\xi^t+\frac{\left|c_{i,j+\frac{1}{2}}-c_{i,j-\frac{1}{2}}^{+}\right|}{\Delta y}\lambda_\eta^t\right)\sqrt{\xi_k^2+\eta_l^2}\geqslant 0$$

or

$$\Delta t\max_{ijkl}\left[\frac{c_{ij}\gamma_t}{\Delta x}+\frac{c_{ij}\gamma_i}{\Delta y}+\left(\frac{\left|c_{i+\frac{1}{2},j}-c_{i-\frac{1}{2},j}^{+}\right|}{\Delta x\Delta\xi}+\frac{\left|c_{i,j+\frac{1}{2}}-c_{i,j-\frac{1}{2}}^{+}\right|}{\Delta y\Delta\eta}\right)\sqrt{\xi_k^2+\eta_l^2}\right]\leqslant 1.\tag{5.12}$$

The quantity $\frac{\left|c_{i+\frac{1}{2},j}-c_{i-\frac{1}{2},j}^{+}\right|}{\Delta x}$ and $\frac{\left|c_{i,j+\frac{1}{2}}-c_{i,j-\frac{1}{2}}^{+}\right|}{\Delta y}$ now represent the wave speed gradients at their smooth points, which have a finite upper bound if we assume $c(\mathbf{x})\in W^{1,\infty}$. The scheme is positive when a hyperbolic type time step constraint (5.12) is satisfied.

6. Numerical examples

In this section we present numerical examples to demonstrate the validity of our scheme and to show the numerical accuracy. In the numerical computations the second order Runge–Kutta time discretization is used.

Since it is difficult to get the exact solution for this problem, we use the numerical solution with the mesh size small enough to represent the exact solution. The immersed interface method for the acoustic wave equations with discontinuous coefficients constructed by Zhang and LeVeque [45] based on the two-dimensional Lax–Wendroff method with space mesh size $h = \frac{\epsilon}{20}$ and $\Delta t = h/2$ are used to solve the system (1.1) in the form

$$\begin{cases} \frac{\partial \mathbf{r}}{\partial t} - \nabla s = 0, \\ \frac{1}{c(\mathbf{x})^2}\frac{\partial s}{\partial t} - \mathrm{div}\mathbf{r} = 0 \end{cases}$$

with $s = \frac{\partial u}{\partial t}, \mathbf{r} = \nabla u$ to get the energy density distribution

$$\mathcal{E}(\mathbf{x}, t) = \frac{1}{2}\frac{1}{c(\mathbf{x})^2}|s|^2 + \frac{1}{2}|\mathbf{r}|^2. \tag{6.1}$$

The numerical energy density is defined as

$$\mathcal{E}_{ij} = \frac{1}{2}\frac{1}{c_{ij}^2}|s_{ij}|^2 + \frac{1}{2}|\mathbf{r}_{ij}|^2, \tag{6.2}$$

where

$$s_{ij} = \frac{1}{\Delta x \Delta y}\int_{x_{i-1/2}}^{x_{i+1/2}}\int_{y_{i-1/2}}^{y_{i+1/2}} s(x, y)\mathrm{d}x\,\mathrm{d}y$$

and $\mathbf{r}_{ij}$ can be defined similarly.

The discrete wave equation is quite dispersive [11], so one needs many grid points per wavelength to compute it. The mesh size $h = \epsilon/20$ is the biggest mesh size we can get satisfactory numerical results for the discrete wave equation.

The limit energy density is the zeroth moment of the density distribution of Liouville equation

$$\mathcal{E}^{(0)}(x, y, t) = \int\int f(x, y, \xi, \eta, t)\mathrm{d}\eta\,\mathrm{d}\xi.$$

We use the super computer at the Tsinghua National Laboratory for Information Science and Technology, which has 512 Itanium 2 64 bit processor. Its peak computational speed is 2.662×10^{13}, the total EMS memory is 1024G, and the storage space is 26T.

Since a spherical wave can hit the interface at any incident angle and the diffraction of a spherical wave is much larger than a plane wave, in following numerical examples, we will choose some spherical waves as the initial data.

We also need to approximate the delta function initial data of the Liouville equation. We use the product of a discrete delta function in 1D [15]:

$$\delta_\omega(x) = \begin{cases} \frac{1}{\omega}(1 - |\frac{x}{\omega}|), & |\frac{x}{\omega}| \leqslant 1, \\ \\ 0, & |\frac{x}{\omega}| > 1 \end{cases} \tag{6.3}$$

with $\omega = \Delta\xi = \Delta\eta$ to regularize the initial data (6.1). (For more recent numerical studies on the approximations of the delta function, see [41,44].)

Then the energy density distribution are recovered by

$$\mathcal{E}_{ij}^{(0)} = \sum_{kl} f_{ijkl}\Delta\xi\Delta\eta. \tag{6.4}$$

We use the L^1-error in the cumulative distribution function (cdf), i.e., the antiderivative of energy density [19]

$$\int_{-\infty}^{+\infty}\int_{-\infty}^{+\infty}\left|\int_{-\infty}^{x}\int_{-\infty}^{y}\left(\mathcal{E}^{(0)}(s,z,t)-\mathcal{E}(s,z,t)\right)\mathrm{d}s\,\mathrm{d}z\right|\mathrm{d}x\,\mathrm{d}y, \tag{6.5}$$

which can be expected to flatten as ϵ is decreased, to measure the weak convergence in the semi-classical limit. Lemma 2.1 in [4] ensures that (6.5) going to zero is equivalent to the weak convergence of $\mathcal{E}^{(0)}(x,y,t)$

Below we denote our scheme by GTD, and the method in [26] by GO. The numerical error comes from the following two parts:

I. The model error: Geometric Theory of Diffraction gives $O(\epsilon^{1/3})$ correction to the zeroth order approximation of the wave equation—the Liouville equation. So the model error between GTD + Liouville equation is $O(\epsilon)$. In addition, there is also error near caustics introduced by the geometrical optics limit which cannot be rescued even with the GTD addition. Our approach improved the error of GO near the interface, but not near caustics.
II. The discrete error of the numerical approximation of the Liouville equation is $O(\sqrt{\Delta x})$ due to the presence of discontinuity in f.

The total error is therefore $\max(\epsilon,\sqrt{\Delta x})$. This means that the errors between the GTD and wave equation, for fixed ϵ, cannot go to 0 once the mesh size is smaller than $O(\epsilon^{4/3})$.

For related model errors, we also refer to a careful numerical study of the error between a high frequency wave in random media and its weakly-coupling limit—a radiative transfer equation [2].

Example 6.1. First, we consider the wave equation in 2D with a **Type B** interface:

$$\begin{cases}\frac{\partial^2 u}{\partial t^2}-c(x,y)^2\Delta u=0,\\ u(0)=4\epsilon e^{i\frac{(x^2+y^2)}{5\epsilon}-300(x+0.3)^2-300y^2},\\ \frac{\partial u}{\partial t}(0)=4e^{i\frac{(x^2+y^2)}{5\epsilon}-300(x+0.3)^2-300y^2}\end{cases} \tag{6.6}$$

with

$$c(x,y)=\begin{cases}2, & \mathcal{F}_{\mathrm{int}}(x,y)>0,\\ 4, & \mathcal{F}_{\mathrm{int}}(x,y)<0.\end{cases}$$

The interface curve $\mathcal{C}$ is given by

$$\mathcal{F}_{\mathrm{int}}(x,y)=(x-1)^2+y^2-1.$$

The corresponding Liouville equation is

$$f_t+\frac{c(x,y)\xi}{\sqrt{\xi^2+\eta^2}}f_x+\frac{c(x,y)\eta}{\sqrt{\xi^2+\eta^2}}f_y-c_x\sqrt{\xi^2+\eta^2}f_\xi-c_y\sqrt{\xi^2+\eta^2}f_\eta=0 \tag{6.7}$$

with initial data

$$f(0,\mathbf{x},\mathbf{v})=8\left[0.16(x+y)^2+\frac{1}{c(x,y)^2}\right]e^{-600(x+0.3)^2-600y^2}\delta(\xi-0.4x)\delta(\eta-0.4y).$$

The computational domain is chosen to be $[x,y,\xi,\eta]\in[-1,1]\times[-1,1]\times[-1,1]\times[-1,1]$. The physically relevant values for the reflection, transmission coefficient $\alpha_{\pm}^{\mathrm{R}}$, $\alpha_{\pm}^{\mathrm{T}}$ are given by (3.4), and the attenuation constant β_{B_1} and diffraction coefficient $\alpha_{B_1}^{\mathrm{D}}$ are given by (3.15) and (3.16), respectively. The time step is chosen as $\Delta t=\frac{1}{4}\Delta x$.

Fig. 4 shows the contour of numerical energy densities $\mathcal{E}^{(0)}=0.05$ and $\mathcal{E}=0.05$ at $t=0.1,0.4$ for $\epsilon=1/4000$. At $t=0.1$, there are only reflected and transmitted waves when waves cross the interface. At $t=0.4$, the *critically diffracted waves* are generated on the interface, and penetrate into the shadow zone of GO—the zone which the waves in GO cannot arrive. The wavefront of GTD is very close to the solution of the wave equation, which shows that GTD can capture the main feature of the diffraction waves, but GO cannot.

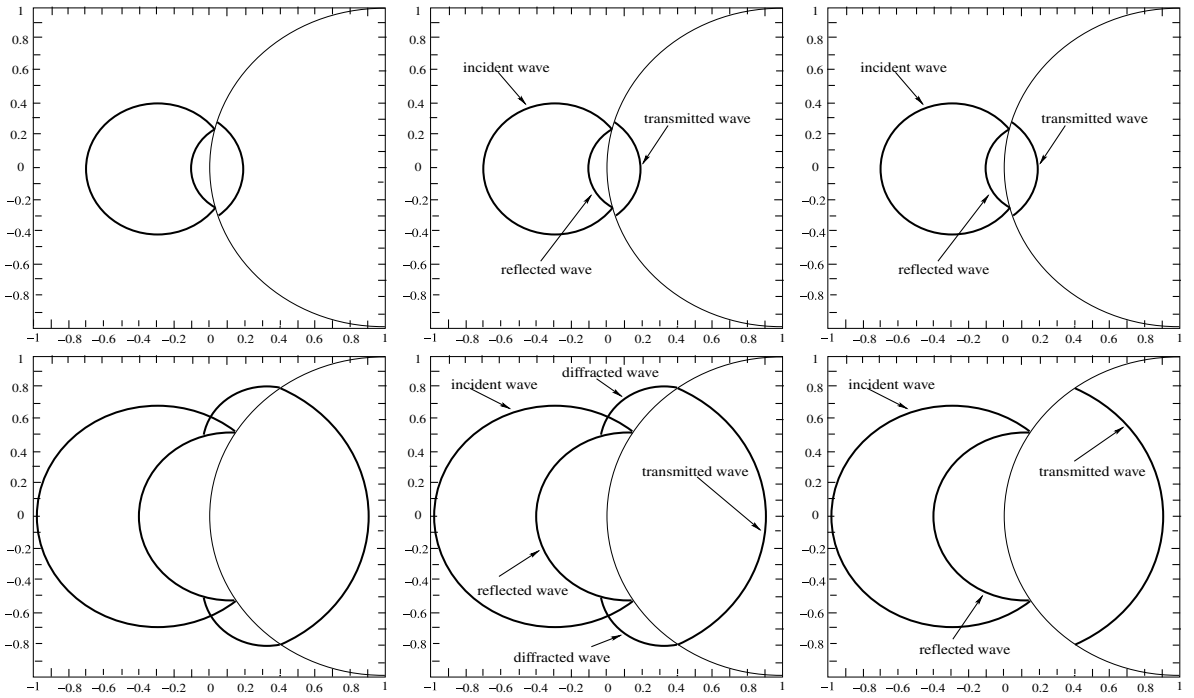

Fig. 4. Example 6.1, contour of energy density $\mathcal{E}$ and $\mathcal{E}^{(0)}$ at $t = 0.1$ (top) and 0.4 (bottom). Left: $\mathcal{E}$; middle: $\mathcal{E}^{(0)}$ by GTD; right: $\mathcal{E}^{(0)}$ by GO.

Fig. 5 depicts the cross-section of numerical energy densities of $\mathcal{E}$ and $\mathcal{E}^{(0)}$ for $y = 0$ and $y = 0.6$ at $t = 0.2$, respectively. One can see that, in the shadow zone (near $x = -0.2, y = 0.6$), the GO solution deviates from the solution of the wave equation more than the GTD solution.

Table 1 presents the numerical errors of the numerical energy density $\mathcal{E}^{(0)}$ computed with different meshes in the phase space at $t = 0.1, 0.2$ and 0.4 with $\epsilon = 1/4000$. The error of GTD is about half of the error of GO when the mesh size is small, and the GTD approximates better for smaller meshes. This is because the diffraction phenomena cannot be captured efficiently unless the mesh size is small enough near the interface. The convergence rate is about first order.

Table 2 shows the error of the numerical energy density $\mathcal{E}^{(0)}$ in the shadow zone $(-0.20 < x < 0.1, |y| > 0.6)$. The GTD solution is a good approximation to the solution wave equation in the shadow zone.

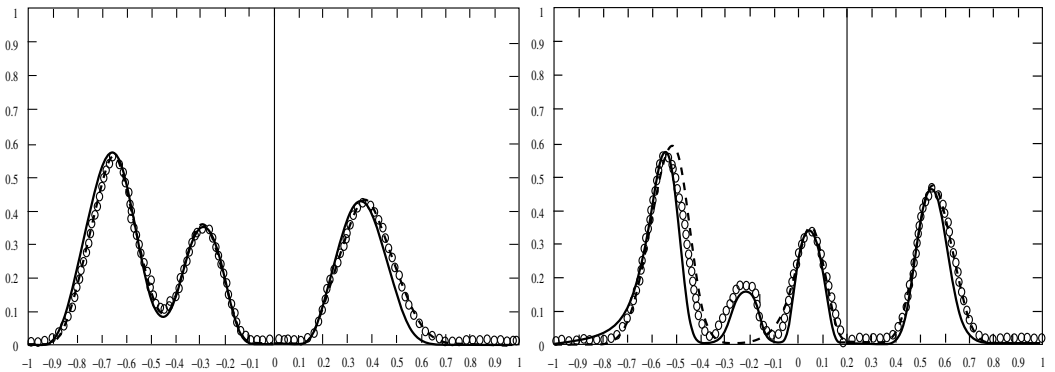

Fig. 5. Example 6.1, the cross-sections of energy density with $\epsilon = 1/4000$ at $t = 0.2$. left, $y = 0$; right, $y = 0.6$. The solid lines are $\mathcal{E}$, '$\circ$' are $\mathcal{E}^{(0)}$ for GTD, and '$-$' are $\mathcal{E}^{(0)}$ for GO.

Table 1
Errors of $\mathcal{E}^{(0)}$ of Example 6.1 for $\epsilon = 1/4000$ on different meshes

Mesh	$100^2 \times 100^2$		$200^2 \times 200^2$		$400^2 \times 400^2$	
	GTD	GO	GTD	GO	GTD	GO
$t = 0.1$	1.0231e−2	1.7023e−2	4.1475e−3	7.9532e−3	2.0332e−3	4.9058e−3
$t = 0.2$	1.3264e−2	2.2044e−2	5.0341e−3	9.8034e−3	3.0134e−3	6.7352e−3
$t = 0.4$	2.1341e−2	3.0108e−2	6.6193e−3	1.2945e−2	4.2324e−3	8.0192e−3

Table 2
Errors of $\mathcal{E}^{(0)}$ of Example 6.1 for $\epsilon = 1/4000$ in the shadow zone

Mesh	$100^2 \times 100^2$ (%)	$200^2 \times 200^2$ (%)	$400^2 \times 400^2$ (%)
$t = 0.1$	9	5.1	2.8
$t = 0.2$	13	7.6	4.1
$t = 0.4$	17.6	10.2	6.1

Table 3 presents the errors of the numerical energy density $\mathcal{E}^{(0)}$ computed with different meshes in phase space at $t = 0.1, 0.2$ and 0.4 with $\epsilon = 1/100$. The wavefronts and cross-section are similar to the case of $\epsilon = 1/4000$. From the numerical results, one can see that GTD is has smaller error than GO. The accuracy is not good as in the case $\epsilon = 1/4000$. This is not surprising since the Liouville equation is the limit of the energy density of wave equation as $\epsilon \to 0$. The Liouville equation is much closer to the original problem when $\epsilon = 1/4000$ than when $\epsilon = 1/100$. Here the main error—the model error which is the difference between the Liouville equation and the wave equation—contributes to the overall errors in Table 3.

Table 4 shows the errors of the GTD solution with $\epsilon = 1/100$ in the shadow zone.

Table 5 presents the errors of the numerical energy density $\mathcal{E}^{(0)}$ computed with different meshes in the phase space at $t = 0.1, 0.2$ and 0.4 with $\epsilon = 1/10,000$. Because the contours and cross-section are similar to the case

Table 3
Errors of $\mathcal{E}^{(0)}$ of Example 6.1 for $\epsilon = 1/100$ on different meshes

Mesh	$100^2 \times 100^2$		$200^2 \times 200^2$		$400^2 \times 400^2$	
	GTD	GO	GTD	GO	GTD	GO
$t = 0.1$	4.2025e−2	5.3112e−2	2.3106e−2	2.7034e−2	9.8915e−3	1.3633e−2
$t = 0.2$	5.3026e−2	5.8054e−2	2.6074e−2	3.1348e−2	1.3015e−2	1.6026e−2
$t = 0.4$	6.7254e−2	7.4029e−2	3.4068e−2	3.7892e−2	1.6864e−2	1.9891e−2

Table 4
Errors of $\mathcal{E}^{(0)}$ of Example 6.1 for $\epsilon = 1/100$ in the shadow zones

Mesh	$100^2 \times 100^2$ (%)	$200^2 \times 200^2$ (%)	$400^2 \times 400^2$ (%)
$t = 0.1$	16	10	7.9
$t = 0.2$	19.1	14.6	12.9
$t = 0.4$	24	18.9	16.4

Table 5
Errors of $\mathcal{E}^{(0)}$ of Example 6.1 for $\epsilon = 1/10,000$ on different meshes

Mesh	$100^2 \times 100^2$		$200^2 \times 200^2$		$400^2 \times 400^2$	
	GTD	GO	GTD	GO	GTD	GO
$t = 0.1$	1.0028e−2	1.5625e−2	3.8054e−3	7.7034e−3	1.3962e−3	3.8368e−3
$t = 0.2$	1.4144e−2	1.7846e−2	4.5656e−3	7.9795e−3	1.7084e−3	4.2396e−3
$t = 0.4$	1.9052e−2	2.5542e−2	6.8032e−3	1.0345e−2	2.4145e−3	5.8347e−3

of $\epsilon = 1/4000$, we omit it. It shows that GTD has smaller errors than GO, but the error of the two method is of the same order. This is partly due to the fact that in this example, the wavelength is very small, so the Liouville equation is a good approximation to the wave equation. From the Geometric Theory of Diffraction, when the wavelength is very small, the diffracted wave, which is of $O(\epsilon^{1/3})$ compared to the incident wave, becomes very weak and decays very fast, and eventually vanishes when $\epsilon \to 0$. As we mention before, we only improve the errors at the interface, and do not improve the errors for the caustics. So there is no big difference between GTD and GO in terms of errors to the wave equation. The convergence rate is of first order.

Table 6 is the errors of GTD solutions for $\epsilon = 1/10,000$ in the shadow region.

The solution of GTD and GO depend on wavelength ϵ. Fig. 6 gives the relation between the error of GTD and GO and the wavelength at $t = 0.2$. One can see that the error of solution of GO is near $O(\epsilon^{1/3})$, and the error of GTD is near $O(\epsilon^{2/3})$ when ϵ is small enough. This is because the diffracted waves decay exponentially, and away from the interface the diffracted waves are very small. Another reason for the error is $O(\epsilon^{2/3})$, not $O(\epsilon)$ is that the discrete error of the numerical approximation of the Liouville equation is of $O(\Delta x)$, which is larger than the model error.

Example 6.2. Consider the wave equation in 2D with a **Type B** interface:

$$\begin{cases} \frac{\partial^2 u}{\partial t^2} - c(x,y)^2 \Delta u = 0, \\ u(0) = 8\epsilon e^{i\frac{(x^2+y^2)}{5\epsilon} - 200(x+0.2)^2 - 200y^2}, \\ \frac{\partial u}{\partial t}(0) = 8e^{i\frac{(x^2+y^2)}{5\epsilon} - 200(x+0.2)^2 - 200y^2} \end{cases} \tag{6.8}$$

with $\epsilon = 1/3000$, and

$$c(x,y) = \begin{cases} 2(1-x)^2, & \mathcal{F}_{\text{int}}(x,y) > 0, \\ 3(x+1)^2, & \mathcal{F}_{\text{int}}(x,y) < 0. \end{cases}$$

The interface curve $\mathcal{C}$ is given by

$$\mathcal{F}_{\text{int}}(x,y) = (x-2)^2 + y^2 - 4.$$

Table 6
Errors of $\mathcal{E}^{(0)}$ of Example 6.1 for $\epsilon = 1/10,000$ in the shadow zones

Mesh	$100^2 \times 100^2$ (%)	$200^2 \times 200^2$ (%)	$400^2 \times 400^2$ (%)
$t = 0.1$	6	4	2.1
$t = 0.2$	9.2	6.4	3.6
$t = 0.4$	15	10	5.6

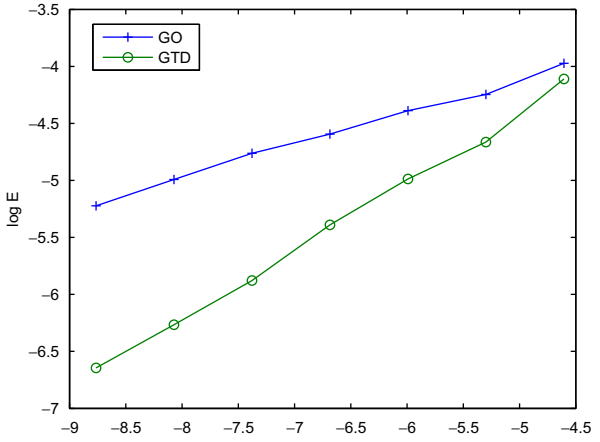

Fig. 6. Relation between $\log_2 E$ and $\log_2 \epsilon$, E is the errors.

The corresponding Liouville equation is (6.7) with initial data

$$f(0,\mathbf{x},\mathbf{v}) = 32\left[0.16(x+y)^2 + \frac{1}{c(x,y)^2}\right]\mathrm{e}^{-400(x+0.2)^2-400y^2}\delta(\xi-0.4x)\delta(\eta-0.4x).$$

The computational domain is chosen to be $[x,y,\xi,\eta]\in[-1,1]\times[-1,1]\times[-1,1]\times[-1,1]$. The physically relevant values for the reflection, transmission coefficient $\alpha_{\pm}^{\mathrm{R}}, \alpha_{\pm}^{\mathrm{T}}$ are given by (3.4), and the attenuation constant β_{B_1} is given by (3.15), β_{B_2} is given by (3.17), the diffraction coefficient $\alpha_{B_1}^{\mathrm{D}}$ is given by (3.16), and $\alpha_{B_2}^{\mathrm{D}}$ is given by (3.18). The time step is chosen as $\Delta t = \frac{1}{4}\Delta x$.

Fig. 7 shows the contour of numerical energy densities $\mathcal{E}^{(0)} = 0.05$ and $\mathcal{E} = 0.05$ at $t = 0.15, 0.4$. At time 0.15, there are only incident, reflected and transmitted waves. At time 0.4, there are *critically diffracted waves* and *tangentially diffracted waves* near the interface. The *critically diffracted wave* arrives firstly at the shadow zone because it travels along the surface of the fast medium, and the *tangentially diffracted wave* travels along the surface of the slow medium for a **Type B** interface.

Fig. 8 depicts the cross-section of the numerical energy densities of $\mathcal{E}$ and $\mathcal{E}^{(0)}$ for $y = 0$ and $y = 0.6$ at $t = 0.25$, respectively. In the shadow zone (near $x = 0,\ y = 0.6$) GTD matches the solution of the wave equation much better than the GO.

Table 7 presents the errors of the numerical energy density $\mathcal{E}^{(0)}$ computed with different meshes in phase space at $t = 0.1, 0.25$ and 0.5.

Table 8 is the errors of the GTD solution in the shadow zones ($|x| \leqslant 0.2,\ |y| \geqslant 0.6$). The GTD solution is a good approximation to the solution wave equation in the shadow zones.

Example 6.3. Consider the 2D wave equation with a **Type A** interface:

$$\begin{cases} \frac{\partial^2 u}{\partial t^2} - c(x,y)^2\Delta u = 0, \\ u(0) = 4\epsilon \mathrm{e}^{\mathrm{i}\frac{x^2+y^2}{4\epsilon}-200(x+0.1)^2-200y^2}, \\ \frac{\partial u}{\partial t}(0) = 4\mathrm{e}^{\mathrm{i}\frac{x^2+y^2}{4\epsilon}-200(x+0.1)^2-200y^2} \end{cases} \tag{6.9}$$

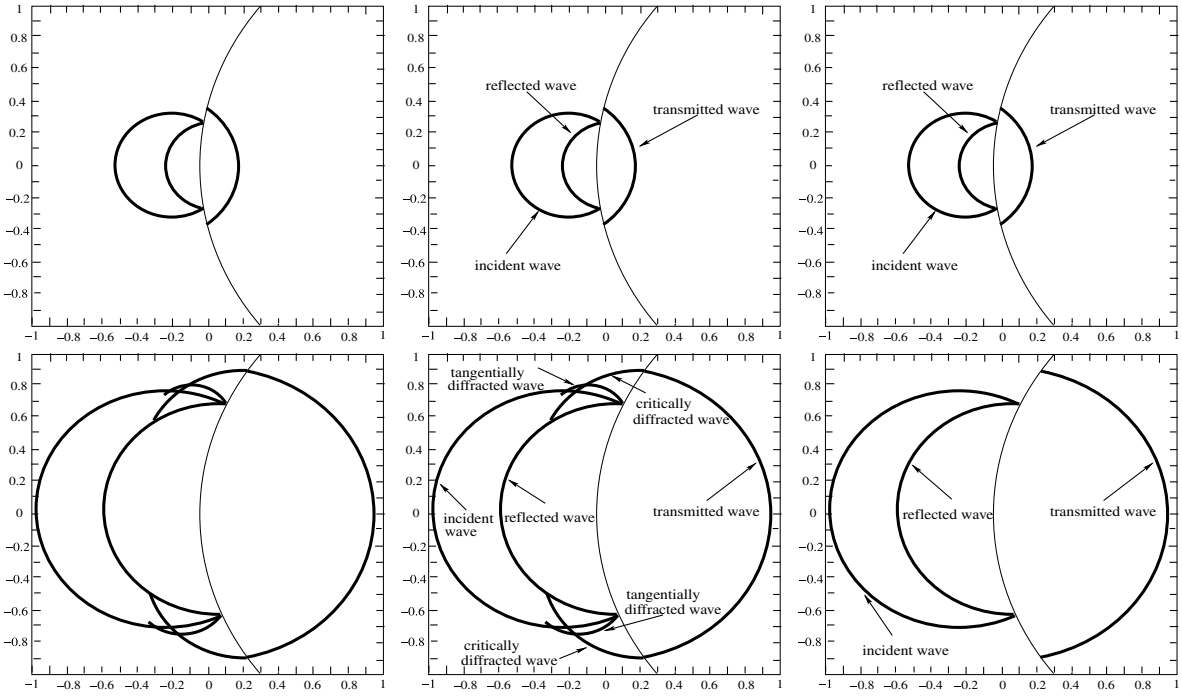

Fig. 7. Example 6.2, contour of energy density $\mathcal{E}$ and $\mathcal{E}^{(0)}$ at $t = 0.15$ (top) and 0.4 (bottom). Left: $\mathcal{E}$; middle: $\mathcal{E}^{(0)}$ by GTD; right: $\mathcal{E}^{(0)}$ by GO.

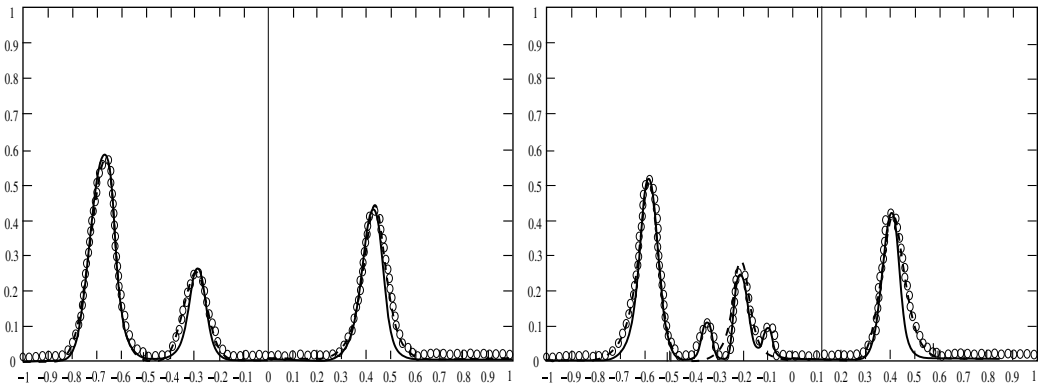

Fig. 8. Example 6.2, cross-section of energy density at $t = 0.25$. left, $y = 0$; right, $y = 0.6$. The solid lines are $\mathcal{E}$, '$\circ$' are $\mathcal{E}^{(0)}$ for GTD, and '$-$' are $\mathcal{E}^{(0)}$ for GO.

Table 7
Errors of $\mathcal{E}^{(0)}$ of Example 6.2 for $\epsilon = 1/3000$ on different meshes

Mesh	$100^2 \times 100^2$		$200^2 \times 200^2$		$400^2 \times 400^2$	
	GTD	GO	GTD	GO	GTD	GO
$t = 0.1$	1.3362e−2	2.0347e−2	4.9452e−3	9.4134e−3	2.4549e−3	5.4152e−3
$t = 0.25$	1.8864e−2	3.0707e−2	6.1103e−3	1.2215e−2	3.0446e−3	6.7035e−3
$t = 0.5$	2.5709e−2	4.1229e−2	9.4044e−3	1.6084e−2	4.8087e−3	9.8704e−3

Table 8
Errors of $\mathcal{E}^{(0)}$ of Example 6.2 for $\epsilon = 1/3000$ in the shadow zones

Mesh	$100^2 \times 100^2$ (%)	$200^2 \times 200^2$ (%)	$400^2 \times 400^2$ (%)
$t = 0.1$	11.1	7.2	4.1
$t = 0.25$	15.3	10.4	5.3
$t = 0.5$	20	14.5	7.6

with $\epsilon = 1/2500$ and

$$c(x,y) = \begin{cases} 2(x-1)^2 + 2(y-1)^2, & \mathcal{F}_{\text{int}}(x,y) < 0, \\ 2(x+2)^2 + 2(y-1)^2, & \mathcal{F}_{\text{int}}(x,y) > 0. \end{cases}$$

The interface curve $\mathcal{C}$ is given by

$$\mathcal{F}_{\text{int}}(x,y) = (x+2.8)^2 + y^2 - 8.84.$$

The corresponding Liouville equation is (6.7) with initial data

$$f(0,\mathbf{x},\mathbf{v}) = 8\left[0.16(x+y)^2 + \frac{1}{c(x,y)^2}\right] \mathrm{e}^{-400(x+0.1)^2 - 400y^2} \delta\Big(\xi - \frac{x}{2}\Big)\delta(\eta - \frac{y}{2}).$$

In this example, the wave speed $c(\mathbf{x})$ depends on x and y. The computational domain is chosen to be $[x,y,\xi,\eta] \in [-0.4,0.4] \times [-0.4,0.4] \times [-0.4,0.4] \times [-0.4,0.4]$. The physically relevant values for the reflection, transmission coefficient $\alpha_{\pm}^{\mathrm{R}}, \alpha_{\pm}^{\mathrm{T}}$ are given by (3.4), and the attenuation constant β_{A_1} is given by (3.6), β_{A_2}, β_{A_3}, is

given by (3.11), the diffraction coefficient $\alpha^{\mathrm{D}}_{A_1}$, $\alpha^{\mathrm{D}}_{A_2}$ and $\alpha^{\mathrm{D}}_{A_3}$ are given by (3.7), (3.13) and (3.14), respectively. The time step is chosen as $\Delta t = \frac{1}{4}\Delta x$.

Fig. 9 shows the contour of numerical energy densities $\mathcal{E}^{(0)} = 0.05$ and $\mathcal{E} = 0.05$ at $t = 0.15, 0.25$. At time 0.15, there is no diffracted wave at the interface. But at time 0.25, there are diffracted waves at both sides of the interface because there will be *critically diffracted wave* in the slow medium and *tangentially diffracted wave* in the fast medium for a **Type A** interface.

Fig. 10 depicts the cross-section of numerical energy densities of $\mathcal{E}$ and $\mathcal{E}^{(0)}$ for $y = 0$ and $y = 0.32$ at $t = 0.25$, respectively. In the shadow zone (near $x = 0.04, y = 0.32$) GTD matches the solution of the wave equation much better than the GO.

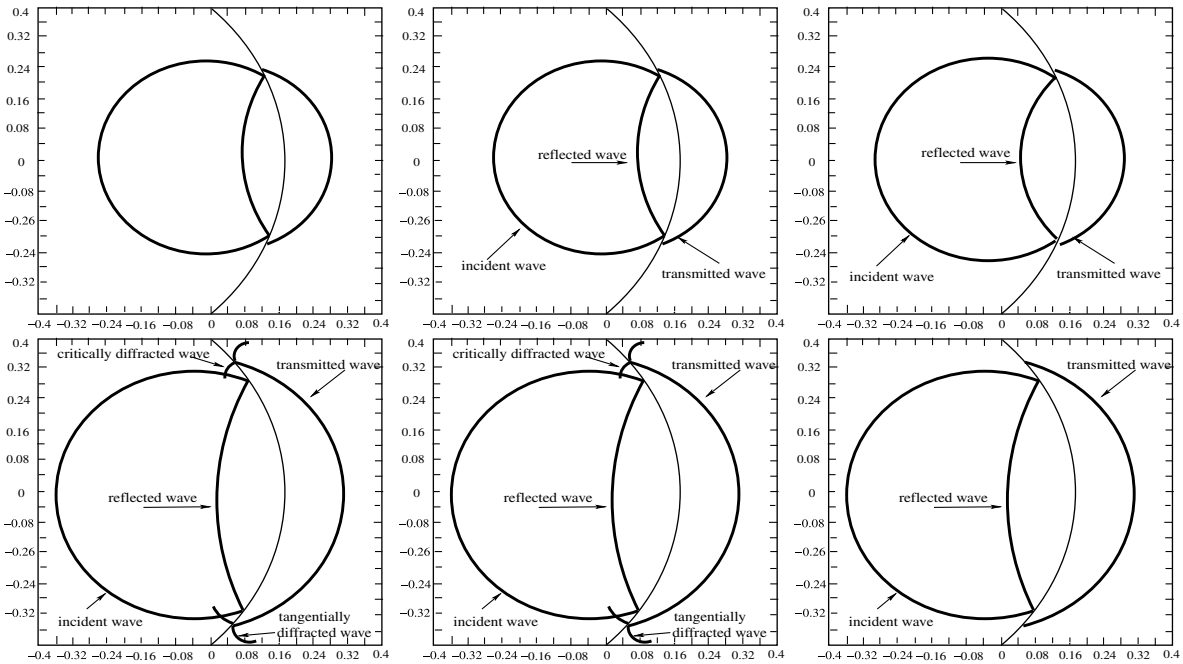

Fig. 9. Example 6.3, contour of energy density $\mathcal{E}$ and $\mathcal{E}^{(0)}$ at $t = 0.1$ (top) and 0.25 (bottom). Left: $\mathcal{E}$; middle: $\mathcal{E}^{(0)}$ by GTD; right: $\mathcal{E}^{(0)}$ by GO.

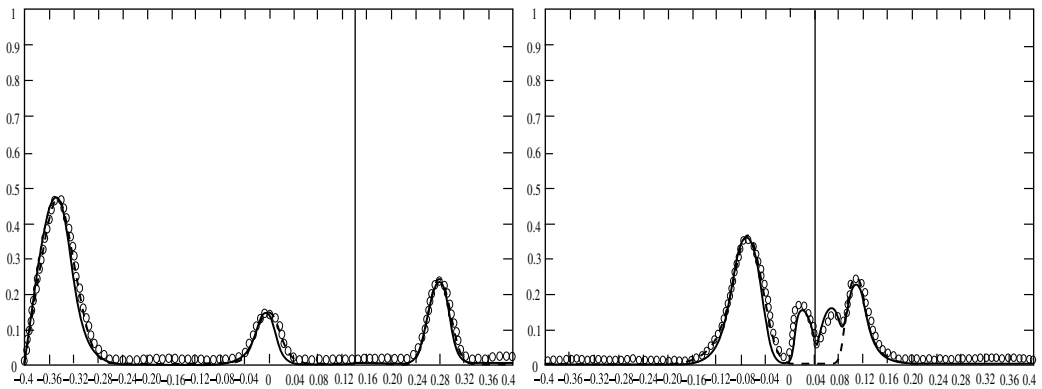

Fig. 10. Example 6.3, cross-section of energy density at $t = 0.25$. left, $y = 0$; right, $y = 0.32$. The solid lines are $\mathcal{E}$, '$\circ$' are $\mathcal{E}^{(0)}$ for GTD, and '$-$' are $\mathcal{E}^{(0)}$ for GO.

Table 9
Errors of $\mathcal{E}^{(0)}$ of Example 6.3 on different meshes

Mesh	$100^2 \times 100^2$		$200^2 \times 200^2$		$400^2 \times 400^2$	
	GTD	GO	GTD	GO	GTD	GO
$t = 0.1$	1.4311e−2	2.4474e−2	7.2045e−3	1.1748e−2	3.5697e−3	6.8014e−3
$t = 0.15$	1.8303e−2	3.1422e−2	8.2147e−3	1.4894e−2	4.0181e−3	7.8085e−3
t=0.25	2.7733e−2	4.0163e−2	9.0408e−3	1.8844e−2	4.5164e−3	9.8143e−3

Table 10
Relative l^1 error of $\mathcal{E}^{(0)}$ for Example 6.3 in the shadow zones

Mesh	$100^2 \times 100^2$ (%)	$200^2 \times 200^2$ (%)	$400^2 \times 400^2$ (%)
$t = 0.1$	11.2	8	4.8
$t = 0.15$	15.4	11.5	6.2
$t = 0.25$	20.8	15.4	8.9

Table 9 shows the errors of the numerical energy density $\mathcal{E}^{(0)}$ computed with different meshes in phase space at $t = 0.1, 0.15$ and 0.25. The convergence rate of GTD is of first order.

Table 10 presents the errors of the numerical energy density $\mathcal{E}^{(0)}$ in the shadow region ($|x| \leqslant 0.12, |y| \geqslant 0.3$).

Remark 1. The typical wave length of visible lights is 400–700 nm, or in the order of 10^{-6} m. To simulate such a high frequency wave in a domain of 1 m requires at least $O(10^6)$ mesh points per spatial dimension. It means $O(10^6)$ meshes in one space dimension, $O(10^{12})$ meshes in two space dimension and $O(10^{18})$ meshes in three dimension. This is simply impossible for today's computational equipments. On the other hand, by using the Liouville equation, although the dimension is doubled, even to resolve the diffraction which is of $O(\epsilon^{1/3}) = O(10^{-2})$, one needs $O(10^8)$ meshes in two space dimension (four dimension in the phase space) and $O(10^{12})$ meshes in three space dimension (six dimension in the phase space). This is a tremendous saving compared to the full simulation based on the original wave equation. Moreover, since the diffraction phenomenon needs to be captured only near the interface, one could use much coarser ($O(1)$) meshes away from the interfaces which will result in a much more significant saving. Thus double the dimension using the Liouville equation provides a much more efficient approach to high frequency waves when the frequency is very high.

7. Conclusion

In this paper, we extend the previous Liouville equation based numerical method in [26] for the simulation of high frequency waves through curved interfaces. The new contribution is to build into the numerical flux the diffraction terms derived from Geometric Theory of Diffraction. Our scheme can effectively compute the diffraction phenomena through curved interfaces, which are generated by the surface waves in addition to partial transmissions and reflections. Numerical experiments show indeed that the diffraction can be captured without resolving the full wavelength of the original wave equation.

In the future we will extend this scheme to other types of interfaces and edges. Another project is to develop an adaptive mesh method that combines a finer mesh near the interface to capture diffraction with a coarser mesh away from the interface, which will reduce the computation cost greatly.

Acknowledgments

The authors thank Tsinghua National Laboratory for Information Science and Technology, China, for computing support. We also thank Beijing International Center for Mathematical Research at Peking University for its support during the Special Semester on Quantunm Kinetic Theory.

Appendix. The detailed algorithm

Firstly, find $C^{\pm}=\left\{(i,j,k,l)\left|\left|\left(\frac{c^{\pm}_{i+1/2,j}}{c^{+}_{i+1/2,j}}\right)^2(\xi'_k)^2+\left[\left(\frac{c^{\pm}_{i+1/2,j}}{c^{+}_{i+1/2,j}}\right)^2-1\right](\eta'_l)^2\right|<\sigma\right\}$, for σ sufficiently small, as the sets of critical angles for $c^{-}_{i+1/2,j}<c^{+}_{i+1/2,j}$ (C^{-}) and $c^{+}_{i+1/2,j}<c^{-}_{i+1/2,j}$ (C^{+}), respectively, and $T=\{k\mid \xi'_k=0\}$, the sets of tangentially incident angle. Then the interface is described parametrically in terms of arclength s in the form

$$x=x(s),\quad y=y(s).$$

For point $(x_i,y_j)=(x(s_p),y(s_p))$, the radius of curvature $a(s_p)$ is given by

$$a(s_p)=a(x_{i+1/2},y_j)=\frac{1}{|x'(s_p)y''(s_p)-x''(s_p)y'(s_p)|}.$$

One can approximate $x'(s),x''(s)$ or evaluate them exactly. $N_{\pm}=\frac{c^{\pm}_{i+1/2,j}}{c^{+}_{i+1/2,j}}$.

The rotation matrix $Q(s_p)=Q(x_{i+1/2},y_j)$ is given by

$$Q(s_p)=\begin{pmatrix}y'(s_p) & -x'(s_p)\\ x'(s_p) & y'(s_p)\end{pmatrix}.$$

- if $\xi'_k>0$,

$f^{-}_{i+\frac12,jkl}=f_{ijkl},\quad (\xi_r,\eta_r)^t=Q^{-1}(s_p)(-\xi'_k,\eta')^t.$

♠ let $\tau^{+}=\left(\frac{c^{+}_{i+\frac12,j}}{c^{-}_{i+\frac12,j}}\right)^2(\xi'_k)^2+\left[\left(\frac{c^{+}_{i+\frac12,j}}{c^{-}_{i+\frac12,j}}\right)^2-1\right](\eta'_l)^2$, if $\tau^{+}>\sigma$ (partial transmission and reflection),

$\xi'_t=\sqrt{\tau^{+}},\quad \eta'_t=\eta'_l,(\xi,\eta)^t=Q^{-1}(s_p)(\xi',\eta')^t.$

♣ if $\xi_{k'}\leqslant\xi_t<\xi_{k'+1}$ for some k', $\eta_{l'}\leqslant\eta_t<\eta_{l'+1}$ for some l', $\xi_{k_1}\leqslant\xi_r<\xi_{k_1+1}$ for some k_1, and $\eta_{l_1}\leqslant\eta_r<\eta_{l_1+1}$ for some l_1,

$$\gamma_i=\frac{|\xi'_k|}{\sqrt{(\xi'_k)^2+(\eta'_l)^2}},\quad \gamma_t=\frac{|\xi'_t|}{\sqrt{(\xi'_k)^2+(\eta'_l)^2}},$$

$$\alpha^{\mathrm{R}}_{+}=\left(\frac{c^{+}_{i+\frac12,j}\gamma_t-c^{-}_{i+\frac12,j}\gamma_i}{c^{+}_{i+\frac12,j}\gamma_t+c^{-}_{i+\frac12,j}\gamma_i}\right),\quad \alpha^{\mathrm{T}}_{+}=1-\alpha^{\mathrm{R}}_{+},$$

$$\begin{aligned}f^{+}_{i+\frac12,jkl}=\alpha^{\mathrm{T}}_{+}\Bigg(&\frac{(\xi_{k'+1}-\xi_t)(\eta_{l'+1}-\eta_t)}{\Delta\xi\Delta\eta}f_{ij,k',l'}+\frac{(\xi_{k'+1}-\xi_t)(\eta_t-\eta_{l'})}{\Delta\xi\Delta\eta}f_{ij,k',l'+1}\\&+\frac{(\xi_t-\xi_{k'})(\eta_t-\eta_{l'})}{\Delta\xi\Delta\eta}f_{ij,k'+1,l'+1}+\frac{(\xi_t-\xi_{k'})(\eta_{l'+1}-\eta_t)}{\Delta\xi\Delta\eta}f_{ij,k'+1,l'}\Bigg)\\&+\alpha^{\mathrm{R}}_{+}\Bigg(\frac{(\xi_{k_1+1}-\xi_r)(\eta_{l_1+1}-\eta_r)}{\Delta\xi\Delta\eta}f_{i+1,j,k_1,l_1}+\frac{(\xi_{k_1+1}-\xi_r)(\eta_r-\eta_{l_1})}{\Delta\xi\Delta\eta}f_{i+1,j,k_1,l_1+1}\\&+\frac{(\xi_r-\xi_{k_1})(\eta_r-\eta_{l_1})}{\Delta\xi\Delta\eta}f_{i+1,j,k_1+1,l_1+1}+\frac{(\xi_r-\xi_{k_1})(\eta_{l_1+1}-\eta_r)}{\Delta\xi\Delta\eta}f_{i+1,j,k_1+1,l_1}\Bigg).\end{aligned}$$

♣ end

♠ if $c^{-}_{i+1/2,j}>c^{+}_{i+1/2,j}$, for a **Type A** interface, $|\tau^{+}|<\sigma$ (**case II**, critical diffraction), $\bar{t}_q=\sum_{j'=j_q}^{j_p}\frac{\sqrt{\Delta x^2+\Delta y^2}}{c^{-}(j')}$, $t^{n_q}\leqslant t_q=t^n-\bar{t}_q\leqslant t^{n_q+1}$ for some n_q, $\bar{t}_{q'}=\sum_{j'=j'_q}^{j_p}\frac{\sqrt{\Delta x^2+\Delta y^2}}{c^{-}(j')}$, and $t^{n_{q'}}\leqslant t_{q'}=t^n-\bar{t}_{q'}\leqslant t^{n_{q'}+1}$ for some $n_{q'}$,

$\xi'_t=\sqrt{\tau^{+}}=0,\quad \eta'_t=\eta',\quad (\xi_t,\eta_t)^t=Q^{-1}(s_p)(0,\eta')^t.$

♠ if $\xi_{k_1}\leqslant\xi_r<\xi_{k_1+1}$ for some k_1, and $\eta_{l_1}\leqslant\eta_r<\eta_{l_1+1}$ for some l_1,

$$\rho_{ij}^{+}=\sqrt{\left(\frac{c_{i+3/2,j}-c_{i+1/2,j}^{+}}{\Delta x}\right)^{2}+\left(\frac{c_{i+1/2,j+1}^{+}-c_{i+1/2,j}^{+}}{\Delta y}\right)^{2}}\Bigg/c_{i+1/2,j}^{+}$$

(or evaluated exactly if possible),

$$\beta_{A_{2,+}}^{ij}=\beta_{A_{3,+}}^{ij}=\frac{\sqrt{3}}{2}q_0(2N_+\epsilon_+)^{-1/3}\left(\frac{1}{a}+\rho_{ij}^{+}\right)^{-2/3}-\frac{1/a+\rho_{ij}^{+}}{\sqrt{1-N_+^2}},$$

$$\alpha_{A_{3,+}}^{\mathrm{D}}(ij)=2^{\frac{3}{2}}\pi^{\frac{1}{2}}\left(\frac{\epsilon_+}{r_{ij}^{+}}\right)^{\frac{1}{2}}\frac{N_+}{(1-N_+^2)^{\frac{1}{2}}}$$

with r_{ij}^{+} the smallest positive number r satisfying

$$2^{3/2}\left(\frac{\pi\epsilon_+}{r}\right)\frac{N_+}{(1-N_+^2)^{1/2}}=\frac{\left|\mathrm{Ai}\left[\epsilon_+^{-2/3}r(2/a+\rho_{ij}^{+})^{\frac{1}{3}}\mathrm{e}^{-\mathrm{i}\pi/3}\right]\right|}{\mathrm{Ai}(0)}$$

and

$$\rho_{ij}^{-}=\sqrt{\left(\frac{c_{i+1/2,j}-c_{i-1/2,j}}{\Delta x}\right)^{2}+\left(\frac{c_{i+1/2,j+1}-c_{i+1/2,j}^{-}}{\Delta y}\right)^{2}}\Bigg/c_{i+1/2,j}^{-}$$

(or evaluated exactly if possible), with $\epsilon_- c^{+}=c^{-}\epsilon_+$,

$$\beta_{A_{1,-}}^{ij}=\frac{\sqrt{3}}{2}q_0(2\epsilon_-)^{-1/3}\left(\frac{1}{a}+\rho_{ij}^{-}\right)^{-2/3}-\frac{1/a+\rho_{ij}^{-}}{\sqrt{N_-^2-1}},$$

$$\alpha_{A_{1,-}}^{\mathrm{D}}(ij)=\frac{\pi^{1/2}\epsilon_-^{\frac{1}{6}}(\rho_{ij}^{-}+1/a)^{-1/3}}{2^{5/6}r_{ij}^{1/2}}\frac{1}{[\mathrm{Ai'}(-q_0)]^2[N_-^2-1]}$$

with r_{ij} the smallest positive number r satisfying

$$r^{\frac{1}{2}}\left|\mathrm{Ai}(-\epsilon_-^{-\frac{2}{3}}2^{\frac{1}{3}}\left(\rho_{ij}^{-}+\frac{1}{a}\right)^{\frac{1}{3}}r+q_0\mathrm{e}^{\frac{\mathrm{i}}{3}\pi})\right|=2^{\frac{1}{6}}\epsilon_-^{\frac{1}{6}}\left(\rho_{ij}^{-}+\frac{1}{a}\right)^{-1/3},$$

$$\begin{aligned}
f_{i+\frac{1}{2},jkl}^{+}(t^n)=\alpha_{A_{3,+}}^{\mathrm{D}}(ij)\sum_{q,m}\alpha_{A_{3,+}}^{\mathrm{D}}(i_q,j_q)\mathrm{e}^{-\sum_{j'=j_q}^{j_p}\beta_{A_{3,+}}(s_{j'})\sqrt{\Delta y^2+\Delta x^2}}\\
\times\Delta y\Delta\xi\left\{\left(\frac{t^{n_q+1}-t_q}{\Delta t}\right)f_{i_q+1,j_q,k_m,l_m}^{n_q}+\left(\frac{t_q-t^{n_q}}{\Delta t}\right)f_{i_q+1,j_q,k_m,l_m}^{n_q+1}\right\}\\
+(1-\alpha_{A_{1,-}}^{\mathrm{D}}(ij))\sum_{q',m'}\alpha_{A_{1,-}}^{\mathrm{D}}(i_{q'},j_{q'})\mathrm{e}^{-\sum_{j'=j_{q'}}^{j_p}\beta_{A_{1,-}}(s_{j'})\sqrt{\Delta x^2+\Delta y^2}}\\
\times\Delta y\Delta\xi\left\{\left(\frac{t^{n_{q'}+1}-t_{q'}}{\Delta t}\right)f_{i_{q'},j_{q'},k_{m'},l_{m'};-}^{n_{q'}}+\left(\frac{t_{q'}-t^{n_{q'}}}{\Delta t}\right)f_{i_{q'},j_{q'},k_{m'},l_{m'};-}^{n_{q'}+1}\right\}\\
+\left(1-\alpha_{A_{3,+}}^{\mathrm{D}}(ij)\right)\left(\frac{(\xi_r-\xi_{k_1})(\eta_r-\eta_{l_1})}{\Delta\xi\Delta\eta}f_{i+1,j,k_1+1,l_1+1}+\frac{(\xi_{k_1+1}-\xi_r)(\eta_r-\eta_{l_1})}{\Delta\xi\Delta\eta}f_{i+1,j,k_1,l_1+1}\right.\\
\left.+\frac{(\xi_{k_1+1}-\xi_r)(\eta_{l_1+1}-\eta_r)}{\Delta\xi\Delta\eta}f_{i+1,j,k_1,l_1}+\frac{(\xi_r-\xi_{k_1})(\eta_{l_1+1}-\eta_r)}{\Delta\xi\Delta\eta}f_{i+1,j,k_1+1,l_1}\right),
\end{aligned}$$

where $(i_q,j_q,k_m,l_m)\in C^{+}$, and $\mathrm{e}^{-\sum_{j'=j_q}^{j_p}\beta_{A_{3,+}}(s_{j'})\sqrt{\Delta y^2+\Delta x^2}}\geqslant\sigma, k_{m'}\in T$, and $\mathrm{e}^{-\sum_{j'=j_{q'}}^{j_p}\beta_{A_{1,-}}(s_{j'})\sqrt{\Delta y^2+\Delta x^2}}\geqslant\sigma$.

♣ if $\xi_{k'} \leqslant \xi_t < \xi_{k'+1}$ for some k', $\eta_{l'} \leqslant \eta_t < \eta_{l'+1}$ for some l',

$$\alpha^{\mathrm{D}}_{A_{2,-}}(ij) = \frac{\pi^{\frac{1}{3}}}{2^{\frac{1}{12}}}\epsilon_-^{\frac{5}{12}} r_{ij}^{-\frac{3}{4}}\left(\rho_{ij}^- + \frac{1}{a}\right)^{-\frac{1}{3}} \frac{N_-}{[\mathrm{Ai}'(-q_0)]^2}\left[N_-^2 - 1\right]^{-\frac{5}{4}}$$

with r_{ij} the smallest positive number r satisfying

$$\left|\mathrm{Ai}\left[\epsilon_-^{-\frac{2}{3}} r\left(\frac{2}{a}\right)^{\frac{1}{3}} \mathrm{e}^{-\frac{i}{3}\pi}\right]\right| = \frac{\pi^{\frac{1}{3}}}{2^{\frac{1}{12}}}\epsilon_-^{\frac{5}{12}} r^{-\frac{3}{4}}\left(\rho_{ij}^- + \frac{1}{a}\right)^{-\frac{1}{3}} N_-\left[N_-^2 - 1\right]^{-\frac{1}{4}},$$

$$\begin{aligned} f^-_{i+\frac{1}{2},jkl;+}(t^n) = {} & \alpha^{\mathrm{D}}_{A_{1,-}}(ij)\sum_{q',m'} \alpha^{\mathrm{D}}_{A_{1,-}}(i_{q'}, j_{q'})\mathrm{e}^{-\sum_{j'=j_{q'}}^{j_p}\beta_{A_{1,-}}(s_{j'})\sqrt{\Delta y^2+\Delta x^2}} \\ & \times \Delta y\Delta\xi\left\{\left(\frac{t^{n_{q'}+1}-t_{q'}}{\Delta t}\right) f^{n_{q'}}_{i_{q'},j_{q'},k_{m'},l_{m'};-} + \left(\frac{t_{q'}-t^{n_{q'}}}{\Delta t}\right) f^{n_{q'}+1}_{i_{q'},j_{q'},k_{m'},l_{m'};-}\right\} \\ & + \alpha^{\mathrm{D}}_{A_{2,-}}(ij)\sum_{q,r} \alpha^{\mathrm{D}}_{A_{2,-}}(i_q, j_q)\mathrm{e}^{-\sum_{j'=j_q}^{j_p}\beta_{A_{2,+}}(s_{j'})\sqrt{\Delta y^2+\Delta x^2}} \\ & \Delta y\Delta\eta\left\{\left(\frac{t^{n_q+1}-t_q}{\Delta t}\right) f^{n_q}_{i_q+1,j_q,k_r,l_r} + \left(\frac{t_q-t^{n_q}}{\Delta t}\right) f^{n_q+1}_{i_q+1,j_q,k_r,l_r}\right\}, \end{aligned}$$

where $(i_q, j_q, k_r, l_r) \in C^+$, $k_{m'} \in T$, $\mathrm{e}^{-\sum_{j'=j_q}^{j_p}\beta_{A_{2,+}}(s_{j'})\sqrt{\Delta y^2+\Delta x^2}} \geqslant \sigma$, and $\mathrm{e}^{-\sum_{j'=j_{q'}}^{j_p}\beta_{A_{1,-}}(s_{j'})\sqrt{\Delta y^2+\Delta x^2}} \geqslant \sigma$.

♣ end

♠ if $c^-_{i+1/2,j} > c^+_{i+1/2,j}$, for a **Type B** interface, $|\tau^+| < \sigma$ (**case I**, critical diffraction), $\bar{t}_q = \sum_{j'=j_q}^{j_p}\frac{\sqrt{\Delta x^2+\Delta y^2}}{c^-(s_{j'})}$, $t^{n_q} \leqslant t_q = t^n - \bar{t}_q \leqslant t^{n_q+1}$ for some n_q, $\xi_{k_1} \leqslant \xi_r < \xi_{k_1+1}$ for some k_1, and $\eta_{l_1} \leqslant \eta_r < \eta_{l_1+1}$ for some l_1,

$$\beta^{ij}_{B_{1,+}} = \frac{\sqrt{3}}{2}q_0(2N_+\epsilon_+)^{-1/3}\left(\frac{1}{a}+\rho^+_{ij}\right)^{-2/3} - \frac{1/a+\rho^+_{ij}}{\sqrt{1-N_+^2}},$$

$$\alpha^{\mathrm{D}}_{B_{1,+}}(ij) = 2^{\frac{3}{2}}\pi^{\frac{1}{2}}\left(\frac{\epsilon_+}{r_{ij}}\right)^{\frac{1}{2}}\frac{N_+}{(1-N_+^2)^{\frac{1}{2}}}$$

with r_{ij} the smallest positive number r satisfying

$$2^{3/2}\left(\frac{\pi\epsilon_+}{r}\right)\frac{N_+}{(1-N_+^2)^{1/2}} = \frac{\left|\mathrm{Ai}\left[\epsilon_+^{-2/3} r(2/a+\rho^+_{ij})^{\frac{1}{3}}\mathrm{e}^{-\mathrm{i}\pi/3}\right]\right|}{\mathrm{Ai}(0)},$$

$$\begin{aligned} f^+_{i+\frac{1}{2},jkl}(t^n) = {} & \alpha^{\mathrm{D}}_{B_{1,+}}(ij)\sum_{q,r}\alpha^{\mathrm{D}}_{B_{1,+}}(i_q, j_q)\mathrm{e}^{-\sum_{j'=j_q}^{j_p}\beta_{B_{1,+}}(s_{j'})\sqrt{\Delta y^2+\Delta x^2}} \\ & \times \Delta y\Delta\eta\left\{\left(\frac{t^{n_q+1}-t_q}{\Delta t}\right) f^{n_q}_{i_q+1,j_q,k_r,l_r} + \left(\frac{t_q-t^{n_q}}{\Delta t}\right) f^{n_q+1}_{i_q+1,j_q,k_r,l_r}\right\} \\ & + \left(1-\alpha^{\mathrm{D}}_{B_{1,+}}(ij)\right)\left(\frac{(\xi_r-\xi_{k_1})(\eta_r-\eta_{l_1})}{\Delta\xi\Delta\eta} f_{i+1,j,k_1+1,l_1+1} + \frac{(\xi_{k_1+1}-\xi_r)(\eta_r-\eta_{l_1})}{\Delta\xi\Delta\eta} f_{i+1,j,k_1,l_1+1}\right. \\ & \left. + \frac{(\xi_{k_1+1}-\xi_r)(\eta_{l_1+1}-\eta_r)}{\Delta\xi\Delta\eta} f_{i+1,j,k_1,l_1} + \frac{(\xi_r-\xi_{k_1})(\eta_{l_1+1}-\eta_r)}{\Delta\xi\Delta\eta} f_{i+1,j,k_1+1,l_1}\right), \end{aligned}$$

where $(i_q, j_q, k_r, l_r) \in C^+$, and $\mathrm{e}^{-\sum_{j'=j_q}^{j_p}\beta_{B_{1,+}}(s_{j'})\sqrt{\Delta y^2+\Delta x^2}} \geqslant \sigma$.

♠ else

$$f^{+}_{i+\frac{1}{2},jkl} = \left(\frac{(\xi_{k_1+1}-\xi_r)(\eta_{l_1+1}-\eta_{1-})}{\Delta\xi\Delta\eta} f_{i+1,j,k_1,l_1} + \frac{(\xi_{k_1+1}-\xi_r)(\eta_r-\eta_{l_1})}{\Delta\xi\Delta\eta} f_{i+1,j,k_1,l_1+1} + \frac{(\xi_r-\xi_{k_1})(\eta_r-\eta_{l_1})}{\Delta\xi\Delta\eta} f_{i+1,j,k_1+1,l_1+1} + \frac{(\xi_r-\xi_{k_1})(\eta_{l_1+1}-\eta_r)}{\Delta\xi\Delta\eta} f_{i+1,j,k_1+1,l_1}\right)$$

with $\xi_{k_1} \leqslant \xi_r < \xi_{k_1+1}$ for some k_1, and $\eta_{l_1} \leqslant \eta_r < \eta_{l_1+1}$ for some l_1.

♠ end

if $\xi'_k = 0$ (tangent diffraction),

for a **Type A** interface (**case I**), if $c^{-}_{i+1/2,j} < c^{+}_{i+1/2,j}$, $\xi_{k'} \leqslant \xi_t < \xi_{k'+1}$ for some k', $\eta_{l'} \leqslant \eta_t < \eta_{l'+1}$ for some l'

$$\beta^{ij}_{A_{1,+}} = \frac{\sqrt{3}}{2} q_0 (2\epsilon_+)^{-1/3} \left(\frac{1}{a}+\rho^{+}_{ij}\right)^{-2/3} - \frac{1/a+\rho^{+}_{ij}}{\sqrt{N_+^2-1}},$$

$$\alpha^{\mathrm{D}}_{A_{1,+}}(ij) = \frac{\pi^{1/2}(\epsilon_+)^{\frac{1}{6}}\left(\rho^{+}_{ij}+1/a\right)^{-1/3}}{2^{5/6} r_{ij}^{1/2}} \frac{1}{[\mathrm{Ai}'(-q_0)]^2[N_+^2-1]},$$

with r_{ij} the smallest positive number r satisfying

$$r^{\frac{1}{2}}\left|\mathrm{Ai}\left(-2^{\frac{1}{3}}\epsilon_+^{\frac{2}{3}}\left(\rho^{+}_{ij}+\frac{1}{a}\right)^{\frac{1}{3}} r + q_0 \mathrm{e}^{\frac{i}{3}\pi}\right)\right| = 2^{\frac{1}{6}}\epsilon_+^{\frac{1}{6}}\left(\rho^{+}_{ij}+\frac{1}{a}\right)^{-1/3}$$

and

$$\beta^{ij}_{A_{2,-}} = \frac{\sqrt{3}}{2} q_0 (2N_-\epsilon_-)^{-1/3} \left(\frac{1}{a}+\rho^{-}_{ij}\right)^{-2/3} - \frac{1/a+\rho^{-}_{ij}}{\sqrt{1-N_-^2}},$$

$$\alpha^{\mathrm{D}}_{A_{2,+}}(ij) = \frac{\pi^{\frac{1}{3}}}{2^{\frac{1}{12}}}\epsilon_+^{\frac{5}{12}} r_{ij}^{-\frac{3}{4}}\left(\rho^{+}_{ij}+\frac{1}{a}\right)^{-\frac{1}{3}} \frac{N_+}{[\mathrm{Ai}'(-q_0)]^2}[N_+^2-1]^{-\frac{5}{4}}$$

with r_{ij} the smallest positive number r satisfying

$$\left|\mathrm{Ai}\left[\epsilon_+^{-\frac{2}{3}} r\left(\frac{2}{a}\right)^{\frac{1}{3}}\mathrm{e}^{-\frac{i}{3}\pi}\right]\right| = \frac{\pi^{\frac{1}{3}}}{2^{\frac{1}{12}}}\epsilon_+^{\frac{5}{12}} r^{-\frac{3}{4}}\left(\rho^{+}_{ij}+\frac{1}{a}\right)^{-\frac{1}{3}} N_+[N_+^2-1]^{-\frac{1}{4}},$$

$$\begin{aligned} f^{+}_{i+\frac{1}{2},jkl;+}(t^n) = {} & \alpha^{\mathrm{D}}_{A_{1,+}}(ij)\sum_{q,m}\alpha^{\mathrm{D}}_{A_{1,+}}(i_q,j_q)\mathrm{e}^{-\sum_{j'=j_q}^{j_p}\beta_{A_{1,+}}(s_{j'})\sqrt{\Delta y^2+\Delta x^2}} \\ & \times \Delta y\Delta\xi\left\{\left(\frac{t^{n_q+1}-t_q}{\Delta t}\right) f^{n_q}_{i_q+1,j_q,k_m,l_m;-} + \left(\frac{t_q-t^{n_q}}{\Delta t}\right) f^{n_q+1}_{i_q+1,j_q,k_m,l_m;-}\right\} \\ & + \alpha^{\mathrm{D}}_{A_{2,+}}(ij)\sum_{q',m'}\alpha^{\mathrm{D}}_{A_{2,+}}(i_{q'},j_{q'})\mathrm{e}^{-\sum_{j'=j_{q'}}^{j_p}\beta_{A_{2,-}}(s_{j'})\sqrt{\Delta y^2+\Delta x^2}} \\ & \times \left\{\left(\frac{t^{n_{q'}+1}-t_{q'}}{\Delta t}\right) f^{n_{q'}}_{i_{q'},j_{q'},k_{m'},l_{m'}} + \left(\frac{t_{q'}-t^{n_{q'}}}{\Delta t}\right) f^{n_{q'}+1}_{i_{q'},j_{q'},k_{m'},l_{m'}}\right\}, \end{aligned}$$

where $(i_{q'}, j_{q'}, k_{m'}, l_{m'}) \in C^-$, $k_m \in T^+$, $\mathrm{e}^{-\sum_{j'=j_{q'}}^{j_p}\beta_{A_{2,-}}(s_{j'})\sqrt{\Delta y^2+\Delta x^2}} \geqslant \sigma$, and $\mathrm{e}^{-\sum_{j'=j_q}^{j_p}\beta_{A_{1,+}}(s_{j'})\sqrt{\Delta y^2+\Delta x^2}} \geqslant \sigma$.

♠ for a **Type B** interface, if $c^{-}_{i+1/2,j} > c^{+}_{i+1/2,j}$ (**case II**),

$$\beta^{ij}_{B_{2,+}} = \frac{\sqrt{3}}{2} q_0 \left(\frac{1}{2\epsilon_+}\right)^{1/3}(\rho^{+}_{ij}+1/a)^{2/3} - \frac{\rho^{+}_{ij}+1/a}{\sqrt{1-N_+^2}},$$

$$\alpha^{\mathrm{D}}_{B_{2,+}}(ij) = \left(\frac{2\pi\epsilon_+}{r_{ij}}\right)^{\frac{1}{2}}\left\{\frac{(1-N_+^4)^{1/2}|\mathrm{Ai}'(q_0\mathrm{e}^{\frac{2}{3}i\pi})|}{\left[(1-N_+^2)^{\frac{1}{2}} - N_+^2(1+N_+^2)^{\frac{1}{2}}\right]\mathrm{Ai}'(q_0)} - \left(\frac{a}{6\epsilon_+}\right)^{\frac{1}{3}}\frac{|\mathrm{Ai}(q_0\mathrm{e}^{\frac{2}{3}i\pi})|}{\mathrm{Ai}'(q_0)}\right\}$$

with r_{ij} the smallest positive number r satisfying

$$\left|\mathrm{Ai}\left[\epsilon_+^{-\frac{2}{3}} r\left(\frac{2}{a}\right)^{\frac{1}{3}} \mathrm{e}^{-\frac{i}{3}\pi}\right]\right| = \left(\frac{2\pi\epsilon_+}{r}\right)^{\frac{1}{2}} \left\{ \frac{(1-N_+^4)^{1/2}\left|\mathrm{Ai}'\left(q_0 \mathrm{e}^{\frac{2}{3}i\pi}\right)\right|}{\left[(1-N_+^2)^{\frac{1}{2}} - N_+^2(1+N_+^2)^{\frac{1}{2}}\right]\mathrm{Ai}'(q_0)} - \left(\frac{a}{6\epsilon_+}\right)^{\frac{1}{3}} \frac{\left|\mathrm{Ai}(q_0 \mathrm{e}^{\frac{2}{3}i\pi})\right|}{\mathrm{Ai}'(q_0)} \right\},$$

$$f^+_{i+\frac{1}{2},jkl;+}(t^n) = \alpha^{\mathrm{D}}_{B_2,+}(ij) \sum_{q,r} \alpha^{\mathrm{D}}_{B_2,+}(i_q, j_q) \mathrm{e}^{-\sum_{j'=j_q}^{j_p} \beta_{B_2,+}(s_{j'})\sqrt{\Delta y^2+\Delta x^2}}$$
$$\times \left\{ \left(\frac{t^{n_q+1}-t_q}{\Delta t}\right) f^{n_q}_{i_q+1,j_q,k_r,l_r;-} + \left(\frac{t_q - t^{n_q}}{\Delta t}\right) f^{n_q+1}_{i_q+1,j_q,k_r,l_r;-} \right\} + \left(1 - \alpha^{\mathrm{D}}_{B_2,+}(ij)\right) f_{i+1,jkl;-},$$

$k_r \in T^+$, $\mathrm{e}^{-\sum_{j'=j_q}^{j_p} \beta_{B_2,+}(s_{j'})\sqrt{\Delta y^2+\Delta x^2}} \geqslant \sigma$,

- if $\xi'_k < 0$,

$$f^+_{i+\frac{1}{2},jkl} = f_{i+1,jkl}, \quad (\xi_r, \eta_{l_r})^t = Q^{-1}(s_p)(-\xi'_k, \eta')^t,$$

♠ let $\tau^- = \left(\frac{c^-_{i+\frac{1}{2},j}}{c^+_{i+\frac{1}{2},j}}\right)^2 (\xi'_k)^2 + \left[\left(\frac{c^-_{i+\frac{1}{2},j}}{c^+_{i+\frac{1}{2},j}}\right)^2 - 1\right](\eta'_l)^2$, if $\tau^- \geqslant \sigma$ (partial transmission and reflection),

$\xi'_t = -\sqrt{\tau^-}$.

♣ if $\xi_{k'} \leqslant \xi_t < \xi_{k'+1}$ for some k', $\eta_{l'} \leqslant \eta_t < \eta_{l'+1}$ for some l', $\xi_{k_1} \leqslant \xi_r < \xi_{k_1+1}$ for some k_1, and $\eta_{l_1} \leqslant \eta_r < \eta_{l_1+1}$ for some l_1,

$$\gamma_t = \frac{|\xi'_t|}{\sqrt{(\xi'_t)^2 + (\eta'_l)^2}}, \quad \gamma_i = \frac{|\xi'_k|}{\sqrt{(\xi'_k)^2 + (\eta'_l)^2}},$$

$$\alpha^{\mathrm{R}}_- = \left(\frac{c^-_{i+\frac{1}{2},j}\gamma_t - c^+_{i+\frac{1}{2},j}\gamma_i}{c^-_{i+\frac{1}{2},j}\gamma_t + c^+_{i+\frac{1}{2},j}\gamma_i}\right), \quad \alpha^{\mathrm{T}}_- = 1 - \alpha^{\mathrm{R}}_-,$$

$$\begin{aligned} f^-_{i+\frac{1}{2},jkl} = \alpha^{\mathrm{T}}_- \Bigg(& \frac{(\xi_{k'+1}-\xi_t)(\eta_{l'+1}-\eta_t)}{\Delta\xi\Delta\eta} f_{i+1,j,k',l'} + \frac{(\xi_{k'+1}-\xi_t)(\eta_t-\eta_{l'})}{\Delta\xi\Delta\eta} f_{i+1,j,k',l'+1} \\ & + \frac{(\xi_t-\xi_{k'})(\eta_t-\eta_{l'})}{\Delta\xi\Delta\eta} f_{i+1,j,k'+1,l'+1} + \frac{(\xi_t-\xi_{k'})(\eta_{l'+1}-\eta_t)}{\Delta\xi\Delta\eta} f_{i+1,j,k'+1,l'} \Bigg) \\ & + \alpha^{\mathrm{R}}_- \Bigg(\frac{(\xi_{k_1+1}-\xi_r)(\eta_{l_1+1}-\eta_r)}{\Delta\xi\Delta\eta} f_{ij,k_1,l_1} + \frac{(\xi_{k_1+1}-\xi_r)(\eta_r-\eta_{l_1})}{\Delta\xi\Delta\eta} f_{ij,k_1,l_1+1} \\ & + \frac{(\xi_r-\xi_{k_1})(\eta_r-\eta_{l_1})}{\Delta\xi\Delta\eta} f_{ij,k_1+1,l_1+1} + \frac{(\xi_r-\xi_{k_1})(\eta_{l_1+1}-\eta_r)}{\Delta\xi\Delta\eta} f_{ij,k_1+1,l_1} \Bigg). \end{aligned}$$

♣ end

♠ if $c^-_{i+1/2,j} < c^+_{i+1/2,j}$, for a **Type A** interface, $|\tau^-| < \sigma$ (**case II**, critical diffraction), $\bar{t}_q = \sum_{j'=j_q}^{j_p} \frac{\sqrt{\Delta x^2+\Delta y^2}}{c^+(s_{j'})}$, $t^{n_q} \leqslant t_q = t^n - \bar{t}_q \leqslant t^{n_q+1}$ for some n_q,

$$\xi'_t = \sqrt{\tau^+} = 0, \quad \eta'_t = \eta', \quad (\xi_t, \eta_t)^t = Q^{-1}(s_p)(0, \eta')^t.$$

♣ if $\xi_{k_1} \leqslant \xi_r < \xi_{k_1+1}$ for some k_1, and $\eta_{l_1} \leqslant \eta_r < \eta_{l_1+1}$ for some l_1,

$$\beta_{A_3,-}(s_p) = \beta^{ij}_{A_3,-} = \frac{\sqrt{3}}{2} q_0 (2N_-\epsilon_-)^{-1/3} \left(\frac{1}{a} + \rho^-_{ij}\right)^{-2/3} - \frac{1/a + \rho^-_{ij}}{\sqrt{1-N_-^2}},$$

$$\alpha^{\mathrm{D}}_{A_3,-}(ij) = 2^{\frac{3}{2}}\pi^{\frac{1}{2}} \left(\frac{\epsilon_-}{r^-_{ij}}\right)^{\frac{1}{2}} \frac{N_-}{(1-N_-^2)^{\frac{1}{2}}}$$

with r_{ij} the smallest positive number r satisfying

$$2^{3/2}\left(\frac{\pi\epsilon_-}{r}\right)\frac{N_-}{(1-N_-^2)^{1/2}}=\frac{\left|\mathrm{Ai}\left[\epsilon_-^{-2/3}r(2/a+\rho_{ij}^-)^{\frac{1}{3}}\mathrm{e}^{-\mathrm{i}\pi/3}\right]\right|}{\mathrm{Ai}(0)}$$

and $t^{n_{q'}}\leqslant t_{q'}=t^n-\bar{t}_{q'}\leqslant t^{n_{q'}+1}$ for some $n_{q'}$,

$$\beta_{A_{1,+}}^{ij}=\frac{\sqrt{3}}{2}q_0(2\epsilon_+)^{-1/3}\left(\frac{1}{a}+\rho_{ij}^+\right)^{-2/3}-\frac{1/a+\rho_{ij}^+}{\sqrt{N_+^2-1}},$$

$$\alpha_{A_{1,+}}^{\mathrm{D}}(ij)=\frac{\pi^{1/2}\epsilon_+^{\frac{1}{6}}(\rho_{ij}^++1/a)^{-1/3}}{2^{5/6}r_{ij}^{1/2}}\frac{1}{[\mathrm{Ai}'(-q_0)]^2[N_+^2-1]}$$

with r_{ij} the smallest positive number r satisfying

$$r^{\frac{1}{2}}\left|\ \mathrm{Ai}\left(-\epsilon_+^{-\frac{2}{3}}2^{\frac{1}{3}}(\rho_{ij}^++\frac{1}{a})^{\frac{1}{3}}r+q_0\mathrm{e}^{\frac{i}{3}\pi}\right)\right|=2^{\frac{1}{6}}\epsilon_+^{\frac{1}{6}}\left(\rho_{ij}^++\frac{1}{a}\right)^{-1/3},$$

$$\begin{aligned}
f^-_{i+\frac{1}{2},jkl}(t^n)=\ &\alpha^{\mathrm{D}}_{A_{3,-}}(ij)\sum_{q,m}\alpha^{\mathrm{D}}_{A_{3,-}}(i_q,j_q)\mathrm{e}^{-\sum_{j'=j_q}^{j_p}\beta_{A_{3,-}}(s_{j'})\sqrt{\Delta y^2+\Delta x^2}}\\
&\times\left\{\left(\frac{t^{n_q+1}-t_q}{\Delta t}\right)f^{n_q}_{i_q,j_q,k_m,l_m}+\left(\frac{t_q-t^{n_q}}{\Delta t}\right)f^{n_q+1}_{i_q,j_q,k_m,l_m}\right\}\Delta y\Delta\xi\\
&+(1-\alpha^{\mathrm{D}}_{A_{1,+}}(ij))\sum_{q',m'}\alpha^{\mathrm{D}}_{A_{1,+}}(i_{q'},j_{q'})\mathrm{e}^{-\sum_{\tau=j_{q'}}^{j_p}\beta_{A_{1,+}}(s_{j'})\sqrt{\Delta y^2+\Delta x^2}}\\
&\times\Delta y\Delta\xi\left\{\left(\frac{t^{n_{q'}+1}-t_{q'}}{\Delta t}\right)f^{n_{q'}}_{i_{q'}+1,j_{q'},k_{m'},l_{m'};-}+\left(\frac{t_{q'}-t^{n_{q'}}}{\Delta t}\right)f^{n_{q'}+1}_{i_{q'}+1,j_{q'},k_{m'},l_{m'};-}\right\}\\
&+\left(1-\alpha^{\mathrm{D}}_{A_{3,-}}(ij)\right)\left(\frac{(\xi_r-\xi_{k_1})(\eta_r-\eta_{l_1})}{\Delta\xi\Delta\eta}f_{i,j,k_1+1,l_1+1}+\frac{(\xi_{k_1+1}-\xi_r)(\eta_r-\eta_{l_1})}{\Delta\xi\Delta\eta}f_{i,j,k_1,l_1+1}\right.\\
&\left.+\frac{(\xi_{k_1+1}-\xi_r)(\eta_{l_1+1}-\eta_r)}{\Delta\xi\Delta\eta}f_{i,j,k_1,l_1}+\frac{(\xi_r-\xi_{k_1})(\eta_{l_1+1}-\eta_r)}{\Delta\xi\Delta\eta}f_{i,j,k_1+1,l_1}\right),
\end{aligned}$$

where $(i_q,j_q,k_m,l_m)\in C^-$, $k_{m'}\in T$, $\mathrm{e}^{-\sum_{j'=j_q}^{j_p}\beta_{A_{3,-}}(s_{j'})\sqrt{\Delta y^2+\Delta x^2}}\geqslant\sigma$ and $\mathrm{e}^{-\sum_{j'=j_{q'}}^{j_p}\beta_{A_{1,}}(s_{j'})\sqrt{\Delta y^2+\Delta x^2}}\geqslant\sigma$.

♣ if $\xi_{k'}\leqslant\xi_t<\xi_{k'+1}$ for some k', $\eta_{l'}\leqslant\eta_t<\eta_{l'+1}$ for some l', and

$$\alpha^{\mathrm{D}}_{A_{2,+}}(ij)=\frac{\pi^{\frac{1}{3}}}{2^{\frac{1}{12}}}\epsilon_+^{\frac{5}{12}}r_{ij}^{-\frac{3}{4}}\left(\rho_{ij}^++\frac{1}{a}\right)^{-\frac{1}{3}}\frac{N_+}{[\mathrm{Ai'}(-q_0)]^2}[N_+^2-1]^{-\frac{5}{4}}$$

with r_{ij} the smallest positive number r satisfying

$$\left|\mathrm{Ai}\left[\epsilon_+^{-\frac{2}{3}}r\left(\frac{2}{a}\right)^{\frac{1}{3}}\mathrm{e}^{-\frac{i}{3}\pi}\right]\right|=\frac{\pi^{\frac{1}{3}}}{2^{\frac{1}{12}}}\epsilon_+^{\frac{5}{12}}r^{-\frac{3}{4}}\left(\rho_{ij}^++\frac{1}{a}\right)^{-\frac{1}{3}}N_+[N_+^2-1]^{-\frac{1}{4}},$$

$$\begin{aligned}
f^+_{i+\frac{1}{2},jkl;+}(t^n)=\ &\alpha^{\mathrm{D}}_{A_{1,+}}(ij)\sum_{q',m'}\alpha^{\mathrm{D}}_{A_{1,+}}(i_{q'},j_{q'})\mathrm{e}^{-\sum_{j'=j_{q'}}^{j_p}\beta_{A_{1,+}}(s_{j'})\sqrt{\Delta y^2+\Delta x^2}}\\
&\times\Delta y\Delta\xi\left\{\left(\frac{t^{n_{q'}+1}-t_{q'}}{\Delta t}\right)f^{n_{q'}}_{i_{q'}+1,j_{q'},k_{m'},l_{m'};-}+\left(\frac{t_{q'}-t^{n_{q'}}}{\Delta t}\right)f^{n_{q'}+1}_{i_{p'}+1,j_{q'},k_{m'},l_{m'};-}\right\}\\
&+\alpha^{\mathrm{D}}_{A_{2,+}}(ij)\sum_{q,r}\alpha^{\mathrm{D}}_{A_{2,+}}(i_p,j_q)\mathrm{e}^{-\sum_{j'=j_q}^{j_p}\beta_{A_{2,-}}(s_{j'})\sqrt{\Delta y^2+\Delta x^2}}\\
&\times\Delta y\Delta\eta\left\{\left(\frac{t^{n_q+1}-t_q}{\Delta t}\right)f^{n_q}_{i_q,j_q,k_r,l_r}+\left(\frac{t_q-t^{n_q}}{\Delta t}\right)f^{n_q+1}_{i_q,j_q,k_r,l_r}\right\},
\end{aligned}$$

where $(i_q, j_q, k_r, l_r) \in C^-$, $k_{m'} \in T$, $\mathrm{e}^{-\sum_{j'=j_q}^{j_p} \beta_{A_2,-}(s_{j'})\sqrt{\Delta y^2+\Delta x^2}} \geqslant \sigma$, and $\mathrm{e}^{-\sum_{j'=j_{q'}}^{j_p} \beta_{A_1,+}(s_{j'})\sqrt{\Delta y^2+\Delta x^2}} \geqslant \sigma$.

♣ end

♠ if $c^-_{i+1/2,j} < c^+_{i+1/2,j}$, for a **Type B** interface, $|\tau^-| < \sigma$ (**case I**, critical diffraction), $\bar{t}_q = \sum_{j'=j_q}^{j_p} \frac{\sqrt{\Delta x^2+\Delta y^2}}{c^+(s_{j'})}$, $t^{n_q} \leqslant t_q = t^n - \bar{t}_q \leqslant t^{n_q+1}$ for some n_q, $\xi_{k_1} \leqslant \xi_r < \xi_{k_1+1}$ for some k_1, and $\eta_{l_1} \leqslant \eta_r < \eta_{l_1+1}$ for some l_1,

$$\beta^{ij}_{B_1,-} = \frac{\sqrt{3}}{2} q_0 (2N_-\epsilon_-)^{-1/3} \left(\frac{1}{a} + \rho^-_{ij}\right)^{-2/3} - \frac{1/a + \rho^-_{ij}}{\sqrt{1-N_-^2}},$$

$$\alpha^{\mathrm{D}}_{B_1,-}(ij) = 2^{\frac{3}{2}} \pi^{\frac{1}{2}} \left(\frac{\epsilon_-}{r_{ij}}\right)^{\frac{1}{2}} \frac{N_-}{(1-N_-^2)^{\frac{1}{2}}}$$

with r_{ij} the smallest positive number r satisfying

$$2^{3/2}\left(\frac{\pi\epsilon_-}{r}\right)\frac{N_-}{(1-N_-^2)^{1/2}} = \frac{\left|\mathrm{Ai}\left[\epsilon_-^{-2/3} r (2/a + \rho^-_{ij})^{\frac{1}{3}} \mathrm{e}^{-\mathrm{i}\pi/3}\right]\right|}{\mathrm{Ai}(0)}.$$

$$\begin{aligned} f^-_{i+\frac{1}{2},jkl}(t^n) = {} & \alpha^{\mathrm{D}}_{B_1,-}(ij) \sum_{q,m} \alpha^{\mathrm{D}}_{B_1,-}(i_q, j_q) \mathrm{e}^{-\sum_{j'=j_q}^{j_p} \beta_{B_1,-}(s_{j'})\sqrt{\Delta y^2+\Delta x^2}} \\ & \times \Delta y \Delta \xi \left\{ \left(\frac{t^{n_q+1} - t_q}{\Delta t}\right) f^{n_q}_{i_q,j_q,k_m,l_m} + \left(\frac{t_q - t^{n_q}}{\Delta t}\right) f^{n_q+1}_{i_q,j_q,k_m,l_m} \right\} \\ & + \left(1 - \alpha^{\mathrm{D}}_{B_1,-}(ij)\right) \left(\frac{(\xi_r - \xi_{k_1})(\eta_r - \eta_{l_1})}{\Delta\xi\Delta\eta} f_{i,j,k_1+1,l_1+1} + \frac{(\xi_{k_1+1} - \xi_r)(\eta_r - \eta_{l_1})}{\Delta\xi\Delta\eta} f_{i,j,k_1,l_1+1} \right. \\ & \left. + \frac{(\xi_{k_1+1} - \xi_r)(\eta_{l_1+1} - \eta_r)}{\Delta\xi\Delta\eta} f_{i,j,k_1,l_1} + \frac{(\xi_r - \xi_{k_1})(\eta_{l_1+1} - \eta_r)}{\Delta\xi\Delta\eta} f_{i,j,k_1+1,l_1} \right), \end{aligned}$$

where $(i_q, j_q, k_m, l_m) \in C^-$, and $\mathrm{e}^{-\sum_{j'=j_q}^{j_p} \beta_{B_1,-}(s_{j'})\sqrt{\Delta y^2+\Delta x^2}} \geqslant \sigma$.

♠ else

$$\begin{aligned} f^-_{i+\frac{1}{2},jkl} = {} & \left(\frac{(\xi_{k_1+1} - \xi_r)(\eta_{l_1+1} - \eta_{1-})}{\Delta\xi\Delta\eta} f_{ijk_1,l_1} + \frac{(\xi_{k_1+1} - \xi_r)(\eta_r - \eta_{l_1})}{\Delta\xi\Delta\eta} f_{ij,k_1,l_1+1} \right. \\ & \left. + \frac{(\xi_r - \xi_{k_1})(\eta_r - \eta_{l_1})}{\Delta\xi\Delta\eta} f_{ij,k_1+1,l_1+1} + \frac{(\xi_r - \xi_{k_1})(\eta_{l_1+1} - \eta_r)}{\Delta\xi\Delta\eta} f_{ij,k_1+1,l_1} \right) \end{aligned}$$

with $\xi_{k_1} \leqslant \xi_r < \xi_{k_1+1}$ for some k_1, and $\eta_{l_1} \leqslant \eta_r < \eta_{l_1+1}$ for some l_1.

♠ end

The fluxes $f^{\pm}_{i,j+\frac{1}{2},kl}$ can be constructed similarly.

Remark 2. In considering diffraction one needs density distribution in several previous time steps. In the first few time steps, we simply omit this term until the first time when diffraction occurs.

References

[1] G. Bal, J.B. Keller, G. Papanicolaou, L. Ryzhik, Transport theory for acoustic waves with reflection and transmission at interfaces, Wave Motion 30 (1999) 303–327.

[2] G. Bal, O. Pinaud, Accuracy of transport models for waves in random media (with O. Pinaud), Wave Motion 43 (7) (2006) 561–578.

[3] L.M. Brekhovskikh, Waves in Layered Media, 2nd ed., Academic Press Inc., New York, 1980.

[4] Y. Brenier, E. Grenier, Sticky particles and scalar conservation laws, SIAM J. Numer. Anal. 38 (1998) 317–2328.

[5] R.N. Buchal, J.B. Keller, Boundary layer problems in diffraction theory, Commun. Pure. Appl. Math. 13 (1960) 85–114.

[6] L.-T. Cheng, H.-L. Liu, S. Osher, Computational high-frequency wave propagation using the level set method, with applications to the semi-classical limit of Schrödinger equations, Commun. Math. Sci. 1 (2003) 593–621.

[7] Y.M. Chen, Diffraction by a smooth transparent object, J. Math. Phys. 5 (6) (1964) 820–832.

[8] Y.M. Chen, Diffraction by a smooth transparent object. II. Diffraction by a cylindrical cavity, J. Math. Phys. 6 (8) (1965) 1332–1333.

[9] L.-T. Cheng, M. Kang, S. Osher, H. Shim, Y.-H. Tsai, Reflection in a level set framework for geometric optics, CMES Comput. Model. Eng. Sci. 5 (2004) 347–360.
[10] B. Cockburn, J. Qian, F. Reitich, J. Wang, An accurate spectral/discontinuous finite-element formulation of a phase space-based level set approach to geometric optics, J. Comput. Phys. 208 (2005) 175–195.
[11] G. Cohen, Higher-Order Numerical Methods for Transient Wave Equations, Springer, Berlin, New York, 2002.
[12] M.G. Crandall, P.-L. Lions, Viscosity solutions of Hamilton–Jacobi equations, Trans. Am. Math. Soc. 277 (1983) 1–42.
[13] B. Engquist, O. Runborg, Computational high frequency wave propagation, Acta Numer. 12 (2003) 181–266.
[14] B. Engquist, O. Runborg, A.-K. Tornberg, High frequency wave propagation by the segment projection method, J. Comput. Phys. 178 (2002) 373–390.
[15] B. Engquist, A.-K. Tornberg, R. Tsai, Discretization of dirac delta functions in level set methods, J. Comput. Phys. 207 (2005) 28–51.
[16] E. Fatemi, B. Engquist, S. Osher, Numerical solution of the high frequency symptotic expansion for the scalar wave equation, J. Comput. Phys. 120 (1995) 145–155.
[17] S. Fomel, J.A. Sethian, Fast phase space computation of multiple arrivals, Proc. Natl. Acad. Sci. USA 99 (11) (2002) 7329–7334.
[18] L. Gosse, Multiphase semiclassical approximation of an electron in a one-dimensional crystalline lattice II. Impurities, confinement and Bloch oscillations, J. Comput. Phys 201 (2004) 344–375.
[19] L. Gosse, N.J. Mauser, Multiphase semiclassical approximation of an electron in a one-dimensional crystalline lattice – III. From ab initio models to WKB for Schrödinger–Poisson, J. Comput. Phys. 211 (2006) 326–346.
[20] S. Jin, X. Li, Multi-phase computations of the semiclassical limit of the Schrödinger equation and related problems: Whitham vs. Wigner, Physics D 182 (2003) 46–85.
[21] S. Jin, X. Liao, A Hamiltonian-preserving scheme for high frequency elastic waves in heterogeneous media, J. Hyperbolic Differ. Eqn. 3 (4) (2006) 741–777.
[22] S. Jin, H.L. Liu, S. Osher, R. Tsai, Computing multi-valued physical observables for high frequency limit of symmetric hyperbolic systems, J. Comput. Phys. 210 (2005) 497–518.
[23] S. Jin, S. Osher, A level set method for the computation of multi-valued solutions to quasi-linear hyperbolic PDEs and Hamilton–Jacobi equations, Commun. Math. Sci. 1 (3) (2003) 575–591.
[24] S. Jin, X. Wen, Hamiltonian-preserving scheme for the Liouville equation with discontinuous potentials, Commun. Math. Sci. 3 (2005) 285–315.
[25] S. Jin, X. Wen, Hamiltonian-preserving scheme for the Liouville equation of geometric optics with discontinuous local wave speeds, J. Comput. Phys. 214 (2006) 672–697.
[26] S. Jin, X. Wen, A Hamiltonian-preserving scheme for the Liouville equation of geometric optics with partial transmissions and reflections, SIAM J. Numer. Anal. 44 (2006) 1801–1828.
[27] S. Jin, X. Wen, Computation of transmissions and reflections in geometric optics via the reduced Liouville equation, Wave Motion 43 (8) (2006) 667–688.
[28] J.B. Keller, Geometric theory of diffraction, J. Opt. Soc. Am. 52 (2) (1962) 116–130.
[29] J.B. Keller, A geometric theory of diffraction, in: L.M. Graves (Eds.), Calculus of Variations and its Applications, Proceedings of Symposia in Applied Math, vol. 8, McGraw-Hill Book Company Inc., New York and American Mathematical Society, Providence, Rhode Island, 1958.
[30] J.B. Keller, R. Lewis, Asymptotic methods for partial differential equations: the reduced wave equation and maxwell's equations, in: D. McLaughlin, J.B. Keller, G. Papanicolaou (Eds.), Surveys in Applied Mathematics, Plenum Press, New York, 1995.
[31] R.J. LeVeque, Finite Volume Methods for Hyperbolic Problems, University Press, Cambridge, 2002.
[32] L. Miller, Refraction of high frequency waves density by sharp interfaces and semiclassical measures at the boundary, J. Math. Pure. Appl. IX 79 (2000) 227–269.
[33] R. Mittra, Topic in Applied Physics: Numerical and Asymptotic Techniques in Electromagnetics, vol. 3, Springer-Verlag, 1975.
[34] I.V. Mukhina, Diffraction by a smooth interface between two inhomogeneous media, J. Math. Sci. 3 (1) (1975) 109–123.
[35] M. Motamed, O. Runborg, A fast phase space method for computing creeping rays, J. Comput. Phys. 219 (2006) 276–295.
[36] M. Motamed, O. Runborg, A multiple-patch phase space method for computing trajectories on manifolds with applications to wave propagation problems, Commun. Math. Sci. 5 (2007) 617–648.
[37] S. Osher, L.T. Cheng, M. Kang, H. Shim, Y.-H. Tsai, Geometric optics in a phase-space-based level set and Eulerian framework, J. Comput. Phys. 179 (2) (2002) 622–648.
[38] L. Ryzhik, G. Papanicolaou, J. Keller, Transport equations for elastic and other waves in random media, Wave Motion 24 (1996) 327–370.
[39] L. Ryzhik, G. Papanicolaou, J. Keller, Transport equations for waves in a half space, Commun. PDE's 22 (1997) 1869–1910.
[40] B.D. Seckler, J.B. Keller, Geometric theory of diffraction in inhomogeneous media, J. Acoust. Soc. Am. 31 (1959) 192–205.
[41] P. Smereka, The numerical approximation of a delta function with application to level set methods, J. Comput. Phys. 211 (2006) 77–90.
[42] C. Sparber, N. Mauser, P.A. Markowich, Wigner functions vs. WKB techniques in multivalued geometric optics, J. Asympt. Anal. 33 (2003) 153–187.
[43] L. Ying, E.J. Candés, Fast Geodesics Computation with the Phase Flow Method, preprint, 2006.
[44] X. Wen, High order numerical methods to a type of delta function integrals, J. Comput. Phys. 226 (2007) 1952–1967.
[45] C. Zhang, R. LeVeque, The immersed interface method for acoustic wave equations with discontinuous coefficients, Wave Motion 25 (1997) 237–263.